Journal of Hydrology 625 (2023) 129970

Contents lists available at ScienceDirect

Journal of Hydrology

journal homepage: www.elsevier.com/locate/jhydrol

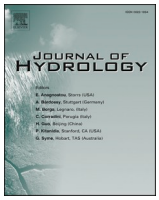

Research papers

Nonstationary stochastic paired watershed approach: Investigating forest harvesting effects on floods in two large, nested, and snow-dominated watersheds in British Columbia, Canada

Robbie S.H. Johnson *, Younes Alila

Forest Resources Management, Faculty of Forestry, University of British Columbia, 2045-2424 Main Mall, Vancouver V6T 1Z4, Canada

ARTICLE INFO

Keywords:
Probabilistic physics
Forest hydrology
Attribution science
Flood Frequency Analysis
Stochastic hydrology
Nonstationarity

ABSTRACT

Drawing on advances in nonstationary frequency analysis and the science of causation and attribution, this study employs a newly developed nonstationary stochastic paired watershed approach to determine the effect of forest harvesting on snowmelt-generated floods. Moreover, this study furthers the application of stochastic physics to evaluate the environmental controls and drivers of flood response. Physically-based climate and time-varying harvesting data are used as covariates to drive the nonstationary flood frequency distribution parameters to detect, attribute, and quantify the effect of harvesting on floods in the snow-dominated Deadman River (878 km^2) and nested Joe Ross Creek (99 km^2) watersheds. Harvesting only 21% of the watershed caused a 38% and 84% increase in the mean but no increase in variability around the mean of the frequency distribution in the Deadman River and Joe Ross Creek, respectively. Consequently, the 7-year, 20-year, 50-year, and 100-year flood events became approximately two, four, six, and ten times more frequent in both watersheds. An increase in the mean is posited to occur from an increase in moisture availability following harvest from suppressed snow interception and increased net radiation reaching the snowpack. Variability was not increased because snowmelt synchronization was inhibited by the buffering capacity of abundant lakes, evenly distributed aspects, and widespread spatial distribution of cutblocks in the watersheds, preventing any potential for harvesting to increase the efficiency of runoff delivery to the outlet. Consistent with similar recent studies, the effect of logging on floods is controlled not only by the harvest rate but most importantly the physiographic characteristics of the watershed and the spatial distribution of the cutblocks. Imposed by the probabilistic framework to understanding and predicting the relation between extremes and their environmental controls, commonly used in the general sciences but not forest hydrology, it is the inherent nature of snowmelt-driven flood regimes which cause even modest increases in magnitude, especially in the upper tail of the distribution, to translate into surprisingly large changes in frequency. Contrary to conventional wisdom, harvesting influenced small, medium, and very large flood events, and the sensitivity to harvest increased with increasing flood event size and watershed area.

1. Introduction

Understanding the relation between forest disturbances and flood response is critical in ensuring effective forest management to minimize the hydrologic effect associated with forest harvesting practices and protect downstream water users. Floods are naturally occurring phenomena, but the magnitude and frequency at which they occur can be exacerbated by land use (e.g., Blum et al., 2020; Hecht & Vogel, 2020; Oudin et al., 2018; Reynard et al., 2001), and/or climate change (e.g., Alfieri et al., 2016; Berghuijs et al., 2017; Milly et al., 2002). Increased flood risk can have severe consequences to downstream lives (e.g., Ashley & Ashley, 2008; Laurance, 2007) and infrastructure (e.g., Downton et al., 2005; François et al., 2019; Kumar et al., 2021), and can negatively impact fluvial ecosystems (e.g., Talbot et al., 2018), degrade water quality (e.g., Alexander et al., 2007), and cause sedimentation issues downstream (e.g., Picchio et al., 2021). In light of emerging questions pertaining to the human influence on the recent devastating November 12–15, 2021, flood event in southwestern BC (Weber, 2021), developing our understanding of the relation between changes in land cover and flooding is now more important than ever.

Currently, there is a general lack of agreement among forest hydrologists on forest covers' ability to mitigate and protect against floods,

* Corresponding author at: 2152 Ridgeway Crescent b1690, Garibaldi Highlands, BC V0N 1T0, Canada.
E-mail address: canmorerobbie@gmail.com (R.S.H. Johnson).

https://doi.org/10.1016/j.jhydrol.2023.129970
Received 2 March 2023; Received in revised form 13 July 2023; Accepted 15 July 2023
Available online 20 July 2023

particularly for large flood events (with return periods > 10 years, e.g., 20, 50, 100 years and beyond) (e.g., Alila et al., 2009, 2010, Alila and Green, 2014a,b; Bathurst, 2014; Birkinshaw, 2014; Bradshaw et al., 2007, 2009; Valentine et al., 1978; van Dijk et al., 2009). In particular, this has spurred considerable confusion and debate among policymakers on whether advocating for an increase in forest cover is an effective natural flood mitigation strategy (e.g., Bradshaw et al., 2009; Carrick et al., 2019).

Disagreement among forest hydrologists on the forest and flood relation is in large part due to differences in how the effect of forest harvesting is measured. Over the last 100 years, most forest hydrology research has adopted a metric, typically applied in paired watershed experiments, where the effect of harvesting on floods has been defined as the difference in magnitude of a flood event when the control and treatment watersheds are subject to the same storm input (for rain dominated regimes), or the same snowmelt season (for snowmelt-dominated regimes), referred to as the chronological pairing (CP) framework. However, Alila et al. (2009) maintained that the effects of harvesting should be measured by the difference in magnitude when control and treatment watershed floods are paired by equal frequency of occurrence, known as the frequency pairing (FP) framework. The different measures are a result of different research questions posed by the investigators, which in turn affects the experimental design meant to control for all possible confounders and isolate the effects of forests on floods.

1.1. CP vs. FP-based paired watershed studies

CP-based studies are dominantly based on the research question: how does the flood response differ in a forested versus unforested watershed, given the same storm input (rain-dominated regimes) or the same snowmelt season (snow-dominated regimes)? FP-based studies, on the other hand, seek to answer the question: how did harvesting affect the magnitude (frequency) of a flood event of the same frequency (magnitude)?

CP studies (e.g., Bathurst et al., 2011, 2020; Dymond et al., 2021) conventionally evaluate the effect of forests on floods by applying the before-after, control-impact (BACI) experimental design. This involves monitoring two, often neighboring watersheds of similar physiography, for several years, known as the calibration period. An empirical relationship between streamflow in both watersheds is developed in the form of a simple linear regression equation, known as the calibration equation. Next, a treatment (e.g., forest harvesting) is applied to one catchment and the calibration equation is used to predict streamflow in the treatment watershed had the treatment not occurred, based on streamflow from the control watershed. The difference between observed and predicted streamflow is then quantified and interpreted as the treatment effect.

Adopted from the wider hydrology and climatology literature (e.g., Howe et al., 1966; Katz, 1993; Katz & Brown, 1992; Salas et al., 2012; Wigley, 1985, 2009), FP-based studies evaluate the treatment effect by comparison of control and treatment flood frequency distributions. In a paired watershed context, FP studies (e.g., Alila et al., 2009; Green & Alila, 2012; Kuraś et al., 2012; Schnorbus & Alila, 2013; Yu & Alila, 2019) evaluate the effect of forest harvesting on floods by comparing differences in pre- and post-harvest flood frequency distributions.

Both CP and FP frameworks alike have been applied in modelling studies where long-term simulated flood data are generated for a given watershed and compared under forested and unforested conditions, provided the same climate inputs. For example, Birkinshaw et al. (2011) applied the SHETRAN model and analyzed its outputs in the CP framework and Schnorbus & Alila, 2013 evaluated outputs from the DHSVM model in the FP framework. In these cases, the fundamental difference between the CP and FP frameworks is not how the data are generated, but rather how the data are analyzed. In the CP-framework, the pre- and post-harvest simulated peak flows are compared one event at a time by linear regression, whereas the FP framework evaluates the effect of harvesting as the difference in the pre- and post-harvest simlutated peak flow frequency distributions.Those that have adopted the CP approach have generally concluded that forests can mitigate small and medium-sized floods in small watersheds, but have no significant influence on the larger events and at larger watershed scales (Calder, 2007; Fahey & Payne, 2017). Some studies have even claimed a threshold beyond which harvesting is thought to no longer affect floods as low as the 2-year (Macdonald & Stednick, 2003; Thomas & Megahan, 1998), 5-year (Beschta et al., 2000), or 10-year (Bathurst et al., 2011; Birkinshaw et al., 2011; Calder, 2007) flood event. Contrarily, outcomes from the emerging FP-based research suggests that forest cover change can affect the magnitude and frequency of large flood events (>10-year return period) (e.g., Alila et al., 2009; Duncan, 1995; Green & Alila, 2012; Kuraś et al., 2012; Reynard et al., 2001; Schnorbus & Alila, 2013). Moreover, based on measured data across a wide range of sample sizes from empirical studies (e.g., Green & Alila, 2012) and simulated flow records from modelling studies (e.g., Birkinshaw et al., 2011, Figure 8, p. 1292; Schnorbus & Alila, 2013), there is mounting evidence indicating that these effects may persist unchecked with increasing event size, although more work is required to validate this prospect.

The process understanding used by advocates of the CP approach to support the contention that larger events are not affected is primarily based on the precept that the forest covers' ability to alleviate moisture via evaporation and interception becomes overwhelmed by the volume of moisture input from a large storm or snowmelt event. Once this capacity is overwhelmed, the amount of water conveyed as runoff would be the same under forested or unforested conditions. Similar reasoning has been restated throughout the forest hydrology literature (e.g., Bathurst et al., 2020, p. 2; DeWalle, 2003, p. 1255), grey literature (e.g., Macdonald & Stednick, 2003, p. 13) and in forest hydrology textbooks (e.g., Cheng, 2012; p. 249). However, stemming from the CP-based research question posed earlier, this reductionist (one event at a time) and deterministic (not invoking the dimension of frequency) line of reasoning leads to an uncontrolled experiment. Therefore, causal inference cannot be established, leading to erroneous conclusions on the relation between forests and floods.

The causes of floods are *multiple and chancy*. Several hydro-meteorological factors control flood generation in snow-dominated hydroclimate regimes. These causal factors include the amount of snow on the ground, energy available to generate snowmelt, rain falling on melting snow, and antecedent soil moisture conditions (AMC). In interior BC, large flood events often coincide with years with exceptional snowpack; however, this is not always the case (Curry & Zwiers, 2018). There are often many causal factors that contribute simultaneously to generating a single flood response (Blum et al., 2020). These factors can work either synergistically to increase the response (e.g., an extreme flood generated by an above-average snow year and rapid spring warming), or antagonistically to dampen the response (e.g., a small flood generated by a normal snow year with gradual spring warming). Conversely, a flood event of the same magnitude could be generated by multiple combinations of these different randomly occurring hydro-meteorological factors.

The probability distribution of floods is conditional on the probability distribution of each hydro-meteorological factor, which collectively, determines the flood regime. In essence, the random combinations and multitude of contributing factors in aggregate, create the stochasticity of floods. This underlying principle necessitates that, to establish a controlled experiment, and hence, the causal inference of forest harvestings' effect on floods, requires that the evaluation be conducted stochastically. Moreover, to causally infer that a change to the flood frequency distribution occurred from a single cause (e.g., forest harvesting), requires an experimental design that fully isolates the treatment effect (Alila et al., 2009) and controls for any confounding variables (Blum et al., 2020). By comparing differences between harvested and unharvested flood frequency distributions (or similarly, flood

frequency curves), the effect of harvesting can be evaluated for floods of the same magnitude, which were likely generated by different flood drivers and/or processes. This is due to the classification of flood events into classes of equal magnitude, regardless of the causal factors that generate floods within that class. No different than the classification of extreme weather events in risk-based event attribution studies (e.g., Stott et al., 2004; van Oldenborgh et al., 2021), each event class represents a magnitude, which occurs at a certain frequency. In aggregate, these classes constitute the hierarchical ranking of the flood frequency distribution. By evaluating how a flood magnitude class has changed in frequency, or conversely, how a frequency class has changed in magnitude, enables all contributing factors to be captured within that change, isolating harvesting as the sole causal factor.

1.2. Nonstationarity and attribution

There has been considerable advancement in the ability to understand historical and predict future flood events in the last several decades. Conventionally, flood frequency analysis (FFA) relied on the stationarity assumption, where the parameters of the frequency distribution of floods, were assumed to remain constant over time (Salas et al., 2018). However, anthropogenic climate and land use change have rendered hydrologic conditions in the past to be unrepresentative of conditions in the future (e.g., Berghuijs et al., 2017; Blum et al., 2020; Kumar et al., 2021). Therefore, the stationarity assumption was deemed to be no longer valid (Milly et al., 2008), and the development of nonstationary methods was required. Nonstationary FFA allows the frequency distribution to vary over time via changes to its parameters.

Allowing the distribution parameters to vary with time alone (e.g., Katz, 2013) is a useful tool for reproducing the behaviour of a historical time-varying flood time series. However, it provides no indication of the underlying drivers of nonstationarity (Chen et al., 2021a). Incorporating physically-based climate covariates into the nonstationary flood frequency distribution models (e.g., Bertola et al., 2021; Chen et al., 2021a; Cheng et al., 2014; Du et al., 2015; El Adlouni et al., 2007; Faulkner et al., 2020; Gilleland & Katz, 2016; Prosdocimi et al., 2015; Shrestha et al., 2017; Su & Chen, 2019; Villarini & Serinaldi, 2012; Villarini & Strong, 2014; Yan et al., 2019; Yu & Alila, 2019) can explain the driver (s) of nonstationarity and improve model fit (Chen et al., 2021a). Additionally, time-varying land-use metrics, such as those representing changes in agricultural area (Slater & Villarini, 2017, 2018), urbanization (Blum et al., 2020; Prosdocimi et al., 2015; Singh & Chinnasamy, 2021), forest cover (McEachran et al., 2021; Yu & Alila, 2019), and even population density (Slater & Villarini, 2017, 2018), have been incorporated as covariates to detect whether changes in land use are acting as nonstationary drivers. However, nonstationary analysis is only recommended when there is physical justification for nonstationarity to be occurring (Montanari & Koutsoyiannis, 2014; Serinaldi et al., 2018). Otherwise, a nonstationary approach can unduly increase uncertainty, particularly for short record lengths. Under such conditions a simpler stationary model is favoured (Serinaldi & Kilsby, 2015).

Nonstationary analyses have considerably advanced our ability to detect trends; however, less attention has been devoted to successfully attributing the underlying causal factors of change (Chen et al., 2021a; Merz et al., 2012). Emerging in parallel with the development of nonstationary analyses, attribution science has been an active area of research over the last 15 years (e.g., Allen & Ingram, 2002; Christidis et al., 2020; Hall & Perdigao, 2021; Otto et al., 2016; Philip et al., 2020; Shepherd, 2016; Stott et al., 2016; van Oldenborgh et al., 2021; Zhai et al., 2018). Largely motivated by furthering an understanding of the influence of anthropogenic climate change on weather and water extremes, attribution studies can be generally classed into two categories: single-event attribution and general causation. Single event attribution studies seek to determine how anthropogenic activities have increased the risk of a single event. For example, investigating the human contribution to the 2003 European heatwave (e.g., Stott et al., 2004). General causation, on the other hand, seeks to address how an intervention, such as climate or land-use change, has influenced the entire distribution of weather and water extremes. For example, a recent increase in high summer temperatures recorded in the United Kingdom prompted Christidis et al. (2020) to determine whether climate change has increased the likelihood of such events from occurring. They found that the likelihood of summers experiencing a temperature exceeding 40 °C, which presently occurred at a 100- to 300-year recurrence interval, would increase in frequency to occur every 3.5 years by 2100. In the context of FFA, general causation involves evaluating how the entire flood regime has been influenced by a single causal factor (e.g., climate change or land use), which becomes complicated as these causal factors can occur simultaneously (Aghakouchak et al., 2020).

1.3. Nonstationary stochastic paired watershed studies

Nonstationary FFA and general causation have been combined to create a nonstationary stochastic paired watershed study. The approach involves selecting a disturbed (e.g., urbanized, harvested, etc.) treatment watershed, and an undisturbed control watershed. The role of the control is to rule out the possibility of a changing frequency distribution in the treatment from anything other than the disturbance. This is achieved by accounting for the natural background climate variability in both treatment and control watersheds by allowing the distribution parameters to vary as a function of local climate factors in the form of covariates. Next, a time-varying disturbance metric is incorporated as a covariate into the nonstationary treatment model. Any additional variability explained by the disturbance metric, which hasn't manifested in the control watershed, can be attributed to the disturbance. To the author's knowledge, this approach has only been applied by Prosdocimi et al. (2015), who detected and attributed the effect of urbanization on floods, and by Yu & Alila (2019) who detected, attributed, and quantified the effect of forest harvesting on floods.

Unlike in conventional stationary paired watershed studies, the control watershed is no longer required to predict flows in the treatment had the disturbance not occurred. The new role of the control enables the size and proximity constraints imposed by the conventional stationary approach to be relaxed. In other words, the control and treatment basins are no longer required to be small and neighboring. For example, the basin pairs used by Prosdocimi et al. (2015) are roughly 30 km apart. Under the nonstationary FP framework, the control and treatment basins must share a similar hydroclimate regime and receive the same synoptic-scale climate inputs but are not required to receive the same meteorological inputs. The assumption of a hydroclimatologically homogenous region is similar to the one often applied in studies investigating the influence of climate on regional trends in, for example, streamflow (e.g., Cunderlik & Burn, 2002; Cunderlik & Ouarda, 2009; Singh & Basu, 2022; Thorne & Woo, 2011; Zhang et al., 2001), meteorology (e.g., Fleming & Whitfield, 2010) or winter snowpack (e.g., Moore & McKendry, 1996; Mote, 2003; Najafi et al., 2017). Thorne & Woo (2011, p. 3077) even stated *"Such regional climatic and hydrological responses to atmospheric forcing are manifested over large scales."* in their investigation of streamflow response to climate variability within the Fraser River Basin. Moreover, the control and treatment basin do not need to share similar physiography. Both the local climate and physiography of each basin are inherently expressed as a signal in their respective flood frequency distributions. Any change in climate over the study period is manifested by the climate covariates in the nonstationary models.

Much like in stochastic stationary paired watershed studies (e.g., Green & Alila, 2012), an understanding of the physics can be evaluated based on harvesting-induced changes to the flood frequency distribution, known as stochastic physics. Stochastic physics involves moving beyond a "statistics only approach" for the purposes of flood prediction, towards using statistics as a tool to better understand the physical processes of flood generation (Dawdy & Gupta, 1997, p.274). Pioneered by

Eagleson (1972), Klemeš (1978), and Yevjevich (1974), evaluating the environmental controls on floods by way of the flood frequency distribution (i.e., stochastic physics) is not a novel concept outside of forest hydrology (e.g., Ayalew & Krajewski, 2017; Blöschl & Sivapalan, 1997). As mentioned previously, the probability distribution of floods is conditional on the probability distribution of each hydro-meteorological factor. Any changes invoked to the distribution of one, or all, of these contributing factors, (e.g., as a result of forest harvesting), will subsequently cause the flood distribution to change. Conversely, evaluating how the flood distribution has changed due to a disturbance, can then be used in conjunction with our current understanding of stand and watershed level physics to infer the cause(s) of that change.

Notwithstanding modelling studies, little research has been conducted to investigate the impact of harvesting on floods in larger watersheds (Slater et al., 2021). Applying outcomes from smaller basins to larger more practical scales is not always valid (e.g., Bertola et al., 2021; Blöschl & Sivapalan, 1995; Lemma et al., 2018). The greatest opportunity unveiled by this novel nonstationary paired watershed framework, is that it allows opportunistic studies to be conducted in a controlled setting outside of conventional experimental watersheds. This opens the doors to both the size and number of watersheds that can now be investigated under a framework aiming at causal inference.

1.4. Research objectives

In the spirit of an approach advocated by Dooge (1986, p. 50), this study uses a top-down inductive approach by developing physically-based, realistic catchment-scale models seeking to uncover catchment-scale hydrologic laws.

The effect of forest harvesting on floods in the Deadman River watershed and nested Joe Ross Creek sub-basin is evaluated using a stochastic nonstationary paired-watershed approach. The purpose of this investigation is to test the following hypotheses:

1. Forest disturbances can affect small (<10-year) and large (>10-year) return periods at the larger (99 and 878 km^2) practical watershed scales, and
2. The drivers of the flood response to disturbances can be inferred by stochastic physics, after accounting for the natural background climate variability.

Additionally, this study is motivated by two primary research objectives: (i) further the application of a newly developed method for detecting, attributing, and quantifying the effect of forest disturbances on the flood regime and (ii) advance the probabilistic physical understanding of the environmental controls that drive the relation between forest disturbances and floods.

2. Study site and watershed description

2.1. Study site

In light of this new framework, forest harvesting effects on floods in the Deadman River watershed, and the nested Joe Ross Creek sub-basin (Fig. 1) can now be investigated for the first time in a controlled experimental setting. The unharvested Big Creek watershed will act as a control for both treatment basins and lies 124 km west of the Deadman River (Fig. 1). Typical of the BC Interior Plateau, all three watersheds have a snow-dominated flow regime, with floods generated by the spring freshet in May, June, or occasionally early July. The Deadman River watershed is located 50 km west of the city of Kamloops on the Thompson Plateau (Province of British Columbia, 2015) and is a tributary to the Thompson River (Fig. 1). It has a drainage area of 878 km^2 upstream of the Water Survey of Canada (WSC) hydrometric station (ID 08LF027). Elevation ranges from 530 m to 1,776 m and the topography is subdued, with 90% of the watershed area above 1,020 m (Fig. 2). Slope and aspects throughout the Deadman River watershed are generally evenly distributed (Fig. 2d). Average annual precipitation is 545 mm (26% as snow) and ranges from 299 mm (16 % as snow) to 569

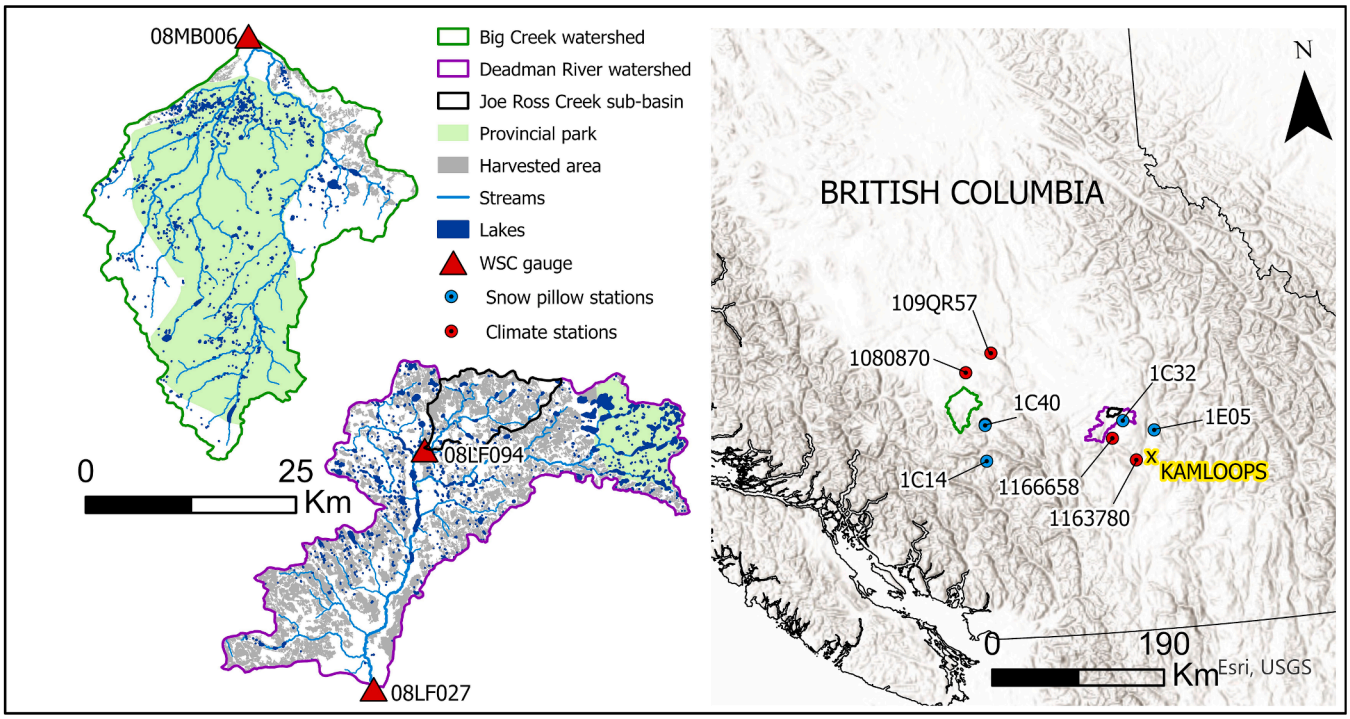

Fig. 1. The Deadman River treatment watershed (purple) and Big Creek control watershed (green) with their stream network and respective Water Survey of Canada gauging station locations. The right plot shows the study basin locations in relation to the snow pillow and climate stations. (For interpretation of the references to color in this figure legend, the reader is referred to the web version of this article.)

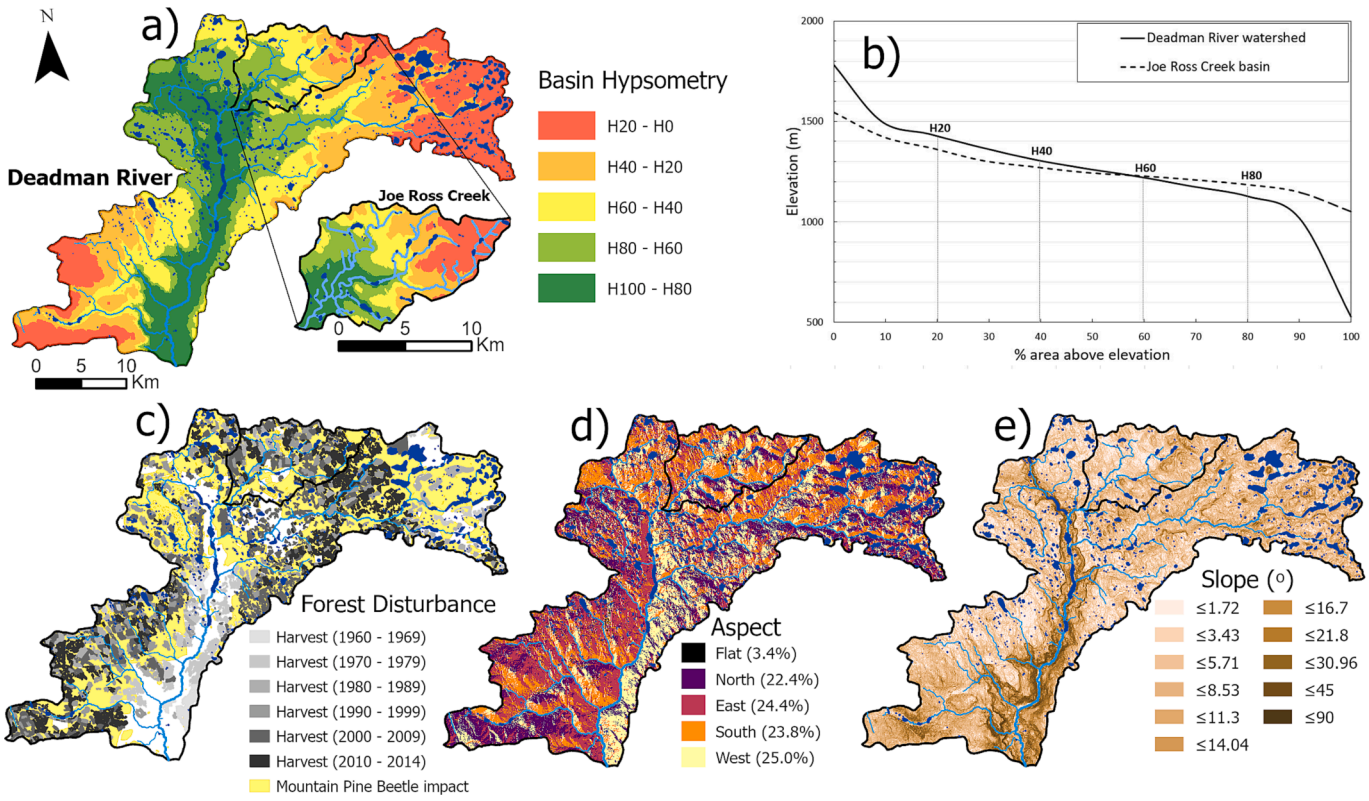

Fig. 2. Physiography of the Deadman River watershed and Joe Ross Creek sub-basin: (a and b) basin hypsometry illustrating the percentage of the basin area that lies above a certain elevation, for example, 60% of the basin area lies above the elevation associated with the H60; (c) harvested area by decade in grey (darker color indicates more recent harvesting) and total area impacted by the mountain pine beetle in yellow; (d) aspect distribution with percentages indicating the portion of the watershed occupied by each aspect; (e) slope map. (For interpretation of the references to color in this figure legend, the reader is referred to the web version of this article.)

mm (45 % as snow), from the lowest to highest elevations, respectively (Wang et al., 2016). It is located within the Interior Douglas-Fir and Sub Boreal Pine-Spruce biogeoclimatic (BEC) zones at lower and mid-elevations, respectively, and the Montane-Spruce zone at higher elevations. Surficial deposits are dominantly post-glacial quaternary till with some glacial lacustrine and alluvial deposits. Additional watershed characteristics are summarized in Table 1.

The watershed lies within the traditional territory of the Skeetchestn Indian Band and has high fisheries values; along its main channel are a series of lakes that act as settling ponds, preventing fine sediment from being delivered to lower reaches used by anadromous fish. Two of the lakes are regulated reservoirs designed to provide downstream flow needs for fisheries and water users during the summer. The storage license associated with these regulated systems (Storage license C047924) allows storage of 2,500 m^3/month at a maximum rate of 100 m^3/day between March 15 and October 31. The daily volume equates to only 0.5 % of the total volume generated by average floods over the study period per day and is therefore expected to have a negligible impact on flood magnitude.

Between 1960 and 2014, a total of 342.6 km^2 or 39 % of the Deadman River watershed area has been clear-cut harvested, largely in response to the widespread mountain pine beetle (MPB) outbreak in 2003 (Fig. 2c). With exception of the valley-bottom and northeast portion of the watershed, which is protected by the Bonaparte Provincial Park, harvesting is generally extensive across the entire watershed area.

Joe Ross Creek is nested within the northern portion of the Deadman River watershed and has an area of 99 km^2 above the WSC flow station (ID 08LF094) located at the mouth (Fig. 1). Elevation in Joe Ross Creek ranges from 1,054 m to 1,559 m and like the Deadman River basin has subdued topography (Fig. 2a, b), although is not characterized by a low-lying valley-bottom (Fig. 2e). The main channel flows from northeast to southwest and is largely dominated by southwest and southern aspects (Fig. 2d). Relative to the Deadman River watershed, the Joe Ross Creek sub-basin receives greater amounts of precipitation annually (508 mm) and a larger proportion in the form of snow (33 %), due to its higher median elevation. Harvesting and MPB impacts in the basin follow a similar temporal trend as the Deadman River, although harvesting levels are higher in Joe Ross Creek (51 %) relative to basin area.

The Big Creek watershed lies 124 km west of the Deadman River basin and is a tributary of the Chilcotin River, located on the Chilcotin Plateau, a western subdivision of the Interior Plateau along the eastern slopes of the Coast Mountains. The watershed has an area of 1,010 km^2 upstream of the WSC stream gauge (ID 08 MB006) with elevation ranging from 1,312 m to 2,989 m. Steep coastal mountains in the headwaters account for 10 % of the watershed area between 2,265 m and 2,989 m, whereas the lower 90 % of the basin area lies between 1,312 m to 2,265 m and is relatively subdued. The basin is characterized by dominantly north, northeast, and northwest facing slopes and is located within the Sub Boreal Pine-Spruce and Montane Spruce BEC zones at lower elevations and within the Engelmann Spruce-Subalpine Fir and Boreal Altai Fescue Alpine zones at higher elevations. Surficial materials are mainly composed of glacial moraine (Fulton, 1975; Valentine et al., 1986).

A significant portion of the watershed is protected by the Big Creek Provincial Park (Fig. 1). Consequently, roughly 5 % of the total basin area has been harvested, most of which is concentrated in lower elevation zones and is therefore not expected to influence floods (Schnorbus & Alila, 2004; Whitaker et al., 2002). The lower one-third of the basin was subject to MPB infestation from 2007 – 2009. However, the recent timing and location of the impact (within 5–7 years of the end of the study period and at low elevations), suggests that the MPB effect on the flow regime is expected to be negligible (Biederman et al., 2015;

Table 1
Watershed characteristics and climate/flow data used for the three study basins: Big Creek (control), Deadman River (treatment), and Joe Ross Creek (treatment).

		Big Creek	Deadman River	Joe Ross Creek
Physiography	Basin area (km^2)	1,011	878	99
	Elevation range (m)	1,312 – 2,980	539 – 1,776	1,054 – 1,559
	Relief (m)	1,668	1,237	505
	Relief ratio	0.034	0.022	0.029
	Stream length (km)	995.4	673.3	86.9
	Drainage density (km/km^2)	0.98	0.77	0.88
	Lake area (km^2)	7.4	24.1	1.3
	Dominant aspects	N/NE/NW	None	SW/S/W
	Mean annual precipitation (mm)	958	454	508
	Precipitation as snow (mm)	610	147	169
	Mean annual temperature (°C)	0.40	3.10	3.00
Land cover	BEC zone[#]	SBPS/MS/ESSF/BAFA	IDF/SBPS/MS	IDF/SBPS/MS
	MPB impacted area (km^2)	332.81	534.27	67.49
	MPB impacted area (%)	32.92	60.84	68.23
	Harvested area (km^2)	49.20	342.55	50.00
	Harvested area (%)	4.95	39.01	50.54
	Portion of MPB area salvage logged (%)		33.17	41.58
	Peak ECA (%)		29.40	38.52
Climate/ flow data	Stream gauge ID	08 MB006	08LF027	08LF094
	Snow pillow station	1C14, 1C40	1C32, 1E05	1C32, 1E05
	Weather station ID	1080870, 1C40P[*], 109QR57	1163790, 1166658	1163790, 1166658
	Years of record	40	40	28

[#] SBPS = Sub-boreal Pine–Spruce; MS = Montane Spruce; ESSF = Engelmann Spruce–Subalpine Fir; BAFA = Boreal Alti Fescue Alpine; IDF = Interior Douglas-fir.
[*] Climate station from the BC Hydro network.

Schnorbus, 2011; Vore et al., 2020). Additionally, Big Creek is currently recognized as a part of the reference hydrometric basin network (as of Feb. 26, 2021), which are a set of gauged stations deemed suitable to climate change studies based on long flow records and minimal human impact (Environment and Climate Change Canada, 2021; Whitfield et al., 2012). Furthermore, a review of satellite imagery following the MPB outbreak revealed that much of the MPB impacted area remains intact, therefore maintaining hydrologic function in the form of snow interception.

2.2. Data

2.2.1. Flood data

Floods in this study are defined as the annual maximum daily flow value (m^3/s); however, only floods generated from snowmelt or rain-on-snow were considered for analysis. Streamflow data were acquired from the Environment and Climate Change Canada Historical Hydrometric Data website (https://wateroffice.ec.gc.ca/mainmenu/historical_data_index_e.html). The flood records span from 1975 to 2014 (40 years) for the Deadman River and Big Creek watersheds, and from 1984 to 2014 (30 years) for the Joe Ross Creek sub-basin. In Big Creek, the largest flow of 1984 occurred from heavy rains during the fall, therefore the largest daily flow value during the freshet was used for that year. Floods from 1991, 1999, 2005, and 2006 in Big Creek were found to be generated by large rain-on-snow (ROS) events and accounted for the largest four flood observations, which deviate from the rest of the empirical flood distribution. To test the nonstationary models to sensitivity from the ROS events, a reduced record was created by omitting these four flows; however, the full record was used for analysis. The largest flood of record in the Deadman River, generated by rain in the days leading to the melt and the largest 3-day warming rate on record was found to be an outlier based on the Grubbs test for one outlier in a data sample (Grubbs, 1950) with a p-value < 0.001. As such, a reduced record was also created for the Deadman River. No outliers were detected in the Joe Ross Creek flood time series; however, two years of flood data were missing resulting in only a 28-year flood record. A similar process of analyzing the nonstationary models using a full and modified record was used by Prosdocimi et al., (2015) and Yu & Alila, (2019). To compare the influence of ROS events on the nonstationary models, both full and reduced records were used for model development; however, the effect of harvesting on floods was quantified using the full record from Big Creek and the reduced record from the Deadman River (with the outlier removed).

2.2.2. Climate data

As mentioned previously, the magnitude of floods in snow-dominated hydroclimate regimes is controlled by several hydro-meteorological factors. These include the amount of snow on the ground, energy available to generate snowmelt, rain falling on melting snow, and antecedent soil moisture conditions (AMC). However, the role of AMC is not expected to vary greatly between freshet years, as soils are likely already saturated when floods occur and are not expected to be a primary predictor of flood response (Curry & Zwiers, 2018; Schnorbus & Alila, 2013). AMC was therefore not included as a covariate in the analysis. Each of the remaining three factors can be represented in the form of climate covariates derived from measured temperature, precipitation, and snow water equivalent (SWE) values, from nearby Environment Canada (EC) weather and BC Government snow pillow stations (Fig. 1).

No single weather station within reasonable proximity of the basins had a complete record spanning the study period, so data from multiple stations in the study area were collated using linear regression to obtain a comprehensive record. For Big Creek, weather data were collated from the North Tyaughton (ID 1C40P) and Big Creek (ID 1080870) stations (R^2 of 0.81), and Wineglass Ranch (ID 109QR57) and Big Creek stations (R^2 of 0.82). SWE data from the North Tyaughton Creek (ID 1C40) was used from 1995 to 2014 and the remaining values were collated using linear regression between the North Tyaughton and Bralorne (ID 1C14) provincial snow pillow stations (R^2 of 0.56). For the Deadman River and Joe Ross Creek, weather data were acquired from the Kamloops Airport (ID 1163780) and Red Lake (ID 1166658) EC stations; however, missing data in 1997 and 2013 was extended by linear regression between the Kamloops airport and Red Lake (ID 1166658) (R^2 of 0.95). SWE data were acquired from the Deadman River (ID 1C32) snow pillow station from 1984 to 2014 and by linear regression between the Knouff Lake (ID 1E05) and Deadman River snow pillow stations from 1975 to 1983 (R^2 of 0.33).

Daily maximum and minimum temperatures were averaged to obtain mean daily temperatures (°C), which were then averaged to determine the 3-day, 5-day and 7-day mean temperature preceding the time of the

peak of the freshet hydrograph. Warming rates (WR) (°C/day) were estimated from mean daily temperatures by calculating the rate at which temperatures increased/decreased during the 3, 7, 15, 30, and 45 days leading up to the time of the flood peak. Daily precipitation (mm) was summed to obtain the total 3-day, 5-day, and 7-day precipitation values. Peak SWE from each snow season preceding the freshet was acquired to represent the amount of snow on the ground in each winter season. Long-term (1981–2010) climate normals, summarized in Table 1, were downscaled by the ClimateBC model developed by Wang et al., (2016).

2.2.3. Forest cover and disturbance data

All forest cover and disturbance data used in this study were sourced from the BC data catalogue (https://catalogue.data.gov.bc.ca/dataset) managed by the BC Ministry of Forests Lands and Natural Resource Operations and Rural Development. The Vegetation Resources Inventory (VRI) 2020 dataset provided forest cover data, including BEC zones, site index, height, age, and species composition. The VRI dataset also provided much of the harvesting data; however, it was incomplete and therefore supplemented by the "Consolidated Cutblocks" and "Results Openings" layers. MPB data were acquired from the Pest Infestation Polygons.

At the watershed scale, harvesting is both spatially and temporally cumulative, whereby the area harvested and time of harvest for each cutblock vary throughout the watershed. To quantify the cumulative impact of harvesting, a metric called Equivalent Clearcut Area (ECA) is introduced to represent the area of each cutblock hydrologically functioning as clearcut (Winkler & Boon, 2017). ECA has been widely used in the forest hydrology literature as a metric to relate forest disturbance impacts to the flow regime (e.g., King, 1989; MacDonald, 2000; Price et al., 2009; Valdal & Quinn, 2011; Varhola et al., 2010a; Winkler et al., 2017) and is calculated as:

$$ECA = A \bullet (1 - HR) \quad (1)$$

where A is the cutblock area and HR is hydrologic recovery ranging from 0 to 1. An HR value of 1 indicates that the cutblock is fully recovered. The sum of ECAs for each cutblock divided by the total watershed area can then be expressed as a percentage representing the portion of the watershed hydrologically functioning as a cutblock at a given point in time. ECAs for each year are then assembled in a time series, which represents the temporal and spatially cumulative impacts of forest harvesting at the watershed scale. ECA can then be readily incorporated as a covariate into the nonstationary modelling procedure (Yu & Alila, 2019). Projected tree heights used in the ECA calculation were obtained from the VRI dataset; however, missing tree height values were calculated based on site index and stand age, using SiteTools 4.1, based on the Table Interpolation Program for Stands Yields (TIPSY, 2021). All forest cover and disturbance data were analyzed using ArcGIS Pro v. 2.8.1.

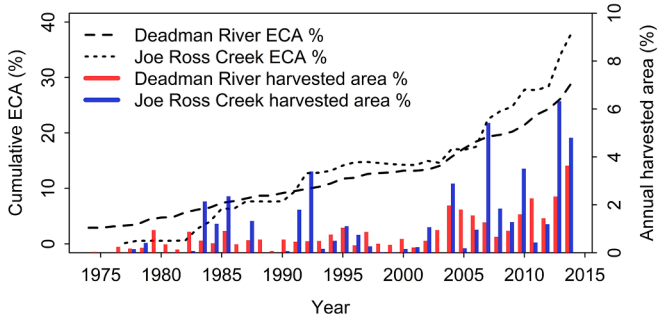

Fig. 3. Harvesting extents throughout the study period (1975 – 2014) in the Deadman River and Joe Ross Creek treatment watersheds. The equivalent clearcut area (ECA) is shown by the dotted and dashed lines and the left y-axis. The percent of the basin area harvested each year is shown by the vertical bars and the right y-axis.

Harvest levels were relatively low in the treatment watersheds until 2003 when salvage harvest operations were implemented in response to the MPB outbreak (Fig. 3). From 2003 to 2014, average ECAs in the Deadman River and Joe Ross Creek basins were 21% and 25%, respectively. ECAs reached 29% in the Deadman River watershed and 39% in the Joe Ross Creek sub-basin by the end of the study period.

3. Methodology

3.1. Conceptual overview

The goal of this study is to use a stochastic nonstationary approach to detect, attribute and quantify the effect of forest harvesting on floods while furthering our understanding of flood drivers using stochastic physics. The attribution framework used in this study falls under the "empirical attribution approach" (Slater et al., 2021, p. 3916), where empirical data are fit to a theoretical frequency distribution to first evaluate whether the data are nonstationary, then determine physical drivers of change by introducing time-varying predictors as covariates into the nonstationary model.

The detection and attribution of the effect of forest harvesting on floods first require that the natural background variability in the flood time series be accounted for, to isolate the effect of harvesting. This is achieved by the careful selection of climate covariates based on a sound apriori understanding of the physical drivers of floods in snowmelt-driven watersheds of Interior BC, as determined from past research (e.g., Curry & Zwiers, 2018; Thorne & Woo, 2011; Whitfield et al., 2010). Climate covariates used in this study include peak annual SWE; warming rate, temperature, and rain preceding the melt; and indices representing the PDO and SOI synoptic-scale teleconnections. Nonstationary models are then developed by allowing the distribution parameters to change over the study period as a function of these climate covariates. Model suitability is determined based on the outcomes of likelihood ratio tests between the stationary and nonstationary model, and Akaike Information Criterion (AIC) scores amongst the nonstationary models.

Next, ECA is introduced as an additional covariate in the final model of the treatment watershed(s) to explain any unaccounted variability. Time is introduced in place of ECA in the control watershed to ensure that, after accounting for the natural climate variability, there is no remaining unexplained variability and there are no trends in the frequency distribution over the study period. This enables any trends detected in the treatment watershed to be solely attributed to harvesting. The final nonstationary model can then be used to evaluate how the magnitude of a certain return period is changing over the study period, by allowing the distribution parameters to change as a function of the covariates. Finally, the effect of harvesting can be quantified by using the long-term average values of the climate covariates, while only allowing the distribution parameters to change as a function of ECA. This enables the evaluation and quantification of changes in magnitude and frequency invoked at different levels of harvesting (ECA).

It is an important reminder that, unlike in conventional paired watershed studies (Andréassian et al., 2012), the control watershed is no longer used to predict floods in the treatment watershed, had logging not occurred. The new role of the control is to rule out a changing frequency distribution from anything other than local (e.g., snow, warming rate, temperature & rain) and synoptic-scale (e.g., PDO & SOI) climate factors. Ruling out any external variability via the nonstationary control model and accounting for the natural background variability in the nonstationary treatment model, allows the effect of harvesting to be isolated and the experiment to be controlled, thereby aiming at a causal inference framework.

3.2. Statistics of extremes framework

Snow-dominated environments typically have a single flood freshet generated by snowmelt in the spring, lending themselves to be evaluated

using the block maxima (BM) approach for modelling hydrologic extremes. BM are typically assumed to originate from a heavy-tailed distribution such as the GEV distribution, which has theoretical justification to be fit to annual maxima (Coles, 2001; Katz, 2013). Furthermore, a recent study intended to identify the best-suited distribution for floods in Canada by Zhang et al. (2020) found that the GEV distribution was the best suited among the distributions examined (GEV, generalized logistic, Pearson type III, and log-Pearson type III).

3.3. GEV distribution

The GEV family of distributions is composed of the Fréchet, Weibull, and Gumbel distributions (Coles, 2001), and is defined by three parameters: the location, scale, and shape, whereby the location provides a measure of central tendency, the scale provides a measure of the deviation around the center of the distribution and the shape determines the overall shape of the distribution (Katz, 2013). Assuming the random variable Q, representing the BM floods, follow a GEV distribution, the probability density function (pdf) and cumulative density function (cdf) of the stationary GEV distribution, as defined by Hosking and Wallis (1997) are:

$$f_q(Q) = \sigma^{(-1)} e^{\left(-(1-\xi)t - e^{(-t)}\right)}, \quad t = \begin{cases} -\xi^{-1} ln(1 - \xi(Q-\mu/\sigma) & when\ \xi \neq 0, \\ (Q-\mu/\sigma) & when\ \xi = 0 \end{cases} \tag{1}$$

$$F_q(Q) = exp\{-e^{-t}\} \tag{2}$$

where μ, σ, and ξ are the location, scale, and shape parameters, respectively. The value of the GEV shape parameter obtained from the empirical data (Q) determines which respective distribution is used in the modelling procedure and hence, the tail behaviour of the distribution (Shrestha et al., 2017). As $-\infty < Q \leq \mu + \frac{\sigma}{\xi}$ if $\xi > 0$ the distribution follows a Fréchet distribution; when $-\infty < Q \leq \infty$ if $\xi = 0$ the distribution has an unbounded thin tail and follows the Gumbel distribution; and when $\mu + \frac{\sigma}{\xi} < Q \leq \infty$ if $\xi < 0$ the distribution has a bounded upper tail and is said to follow the Weibull distribution (Coles, 2001; Katz, 2013; Katz et al., 2002). The cdf of the GEV distribution, calculated in equation (2) is of particular interest as it can be used to determine the return levels of floods, where p is the probability associated with the quantile and $1/p$ is the return period.

Under the conventional stationary approach, the data are assumed to be independent and identically distributed (Salas et al., 2018). However, in the case of nonstationary analyses, the data are assumed to be independent but not necessarily identically distributed. This is because the parameters describing the frequency distribution are modelled to change with time, or other time-varying covariates (e.g., Katz et al., 2002; Salas et al., 2018).

3.4. Parameter estimation

The maximum likelihood (ML) approach to estimate the distribution parameters is widely applied in nonstationary flood frequency analysis (e.g., Prosdocimi et al., 2015; Salas et al., 2018; Strupczewski et al., 2001) as it readily allows covariates to be incorporated into the nonstationary models (Gado & Nguyen, 2016). The location, scale, and shape parameters of the GEV distribution were therefore estimated from the empirical BM flood time series using ML (Coles, 2001).

Denoted by $L(\mu, \sigma, \xi; Q)$, where $Q = (Q_1, \cdots, Q_m)$ is a vector of M block maxima, the likelihood function provides a measure of how likely the observed block maxima Q are of the unknown GEV parameters μ, σ, and ξ. The values of the parameters μ, σ, and ξ that maximize the likelihood function are known as the maximum likelihood estimates (MLEs). It is more convenient to work with the log-likelihood function (Katz, 2013), which can be maximized to obtain the MLEs for the parameters of the GEV distribution with $\xi \neq 0$ by deriving equation (1) as:

$$\mathbf{ln}\boldsymbol{L}(\boldsymbol{\mu}, \boldsymbol{\sigma}, \boldsymbol{\xi}; \boldsymbol{Q}) = \mathbf{ln}\boldsymbol{f}(\boldsymbol{\mu}, \boldsymbol{\sigma}, \boldsymbol{\xi}; \boldsymbol{Q}_1) + \cdots + \mathbf{ln}\boldsymbol{f}(\boldsymbol{\mu}, \boldsymbol{\sigma}, \boldsymbol{\xi}; \boldsymbol{Q}_m) \tag{3}$$

with respect to μ, σ, and ξ. This equation can be simplified as:

$$\mathbf{ln}\boldsymbol{L}(\boldsymbol{\mu}, \boldsymbol{\sigma}, \boldsymbol{\xi}; \boldsymbol{Q}) = \sum_{i=1}^{M} \mathbf{ln}\boldsymbol{f}(\boldsymbol{\mu}, \boldsymbol{\sigma}, \boldsymbol{\xi}; \boldsymbol{Q}_i) \tag{4}$$

It is also more convenient to minimize the negative log-likelihood (nllh) function rather than maximize the log-likelihood function (Katz, 2013). The nllh function $\ln L(\mu, \sigma, \xi; Q)$ can be written as:

$$\mathbf{ln}\boldsymbol{L}(\boldsymbol{\mu}, \boldsymbol{\sigma}, \boldsymbol{\xi}; \boldsymbol{Q}) = -\boldsymbol{M}\mathbf{ln}\boldsymbol{\sigma} \sum_{i=1}^{M} \{\boldsymbol{t}_i(1 - \boldsymbol{\xi}) + \boldsymbol{e}^{-\boldsymbol{t}_i}\} \tag{5}$$

$$t_i = -\xi^{-1} \ln\left(1 - \frac{\xi(Q_i - \mu)}{\sigma}\right)$$

Equation (5) can be adapted for the nonstationary case where one or more of the model parameters are defined as a function changing linearly with a covariate x. For example, if μ were modelled as a linear function of covariate ×, $\mu(x) = \mu_0 + \mu_1 \bullet x$ then the nllh function would now be $-\ln L(\mu(x), \sigma, \xi; Q)$ with the optimization problem minimizing the nllh to four parameters rather than three parameters in the stationary case. Following Katz (2013), equation (5) can be modified for the location parameter as a function of a covariate × as:

$$\mathbf{ln}\boldsymbol{L}(\boldsymbol{\mu}_0, \boldsymbol{\mu}_1, \boldsymbol{\sigma}, \boldsymbol{\xi}; \boldsymbol{Q}, \boldsymbol{x}) = -\boldsymbol{M}\mathbf{ln}\boldsymbol{\sigma} \sum_{i=1}^{M} \{\boldsymbol{t}_i(1 - \boldsymbol{\xi}) + \boldsymbol{e}^{-\boldsymbol{t}_i}\} \tag{6}$$

$$t_i = -\xi^{-1} \ln\left(1 - \frac{\xi(Q_i - \mu_0 - \mu_1 x_i)}{\sigma}\right)$$

If both the location and scale parameters were each modelled as a function of a single covariate, then five parameters would have to be optimized, for example: $\mu_0, \mu_1, \sigma_0, \sigma_1$ and ξ.

Unlike the location and scale parameters, the shape parameter remains unchanged throughout the nonstationary modelling due to computational uncertainties and instability when fitting the distribution (Cannon, 2010; Coles, 2001; Katz et al., 2002; Prosdocimi et al., 2015; Shrestha et al., 2017; Villarini et al., 2018). The shape parameter is rarely made a function of covariates as it is difficult to estimate with precision even in the stationary case (Salas et al., 2018). However, recent studies have shown that the shape parameter may change in response to forest harvesting (McEachran et al., 2021). Following similar studies (e.g., Katz, 2013; Li & Tan, 2015; Prosdocimi et al., 2015; Tan-Soo et al., 2016), and to reduce model complexity, the location and scale parameters are assumed to be linearly related to the covariates, although non-linear (i.e., quadratic) relations can also be modelled (e.g., El Adlouni et al., 2007).

3.5. Model evaluation

To develop an understanding of the physical drivers of floods in the control and treatment watersheds, it is necessary to determine which covariates, or combination of covariates, result in the best-suited model. Furthermore, as covariates are added throughout the modelling procedure, it is necessary to determine whether the addition of a new covariate improves the model performance (i.e., increases the amount of natural background variability in the flood time series explained by the model). Model suitability is determined by two approaches. The first is to perform a likelihood ratio test which allows for formal hypothesis testing between two models but requires that the models be nested (Coles, 2001). The second is to compare the AIC score between two models, which does not require that they be nested, but does not allow for formal hypothesis testing (Coles, 2001). A lower AIC score indicates a superior model. Both approaches rely on the nllh values calculated in equations (5) and (6).

AIC scores are generated by penalizing the minimized nllh function

based on the number of parameters. This accounts for smaller nllh values inherently associated with a model with more parameters, regardless of the relevance of the covariate, which helps reduce the risk of overfitting. For smaller sample sizes ($n < 40$), it is recommended to use the small sample criterion AIC_c in place of AIC, which further penalizes models with a greater number of parameters (Anderson & Burnham, 2002; Burnham & Anderson, 2004). Additionally, as the number of covariates used in the modelling procedure increases, so does the possibility of reaching a lack of convergence, resulting in a non-optimum point under MLE (Restrepo & Bras, 1985), in which case the models are invalid (Anderson & Burnham, 2002).

3.6. Model development

Preliminary models were developed to determine, for the single climate-controlling factors (e.g., precipitation) one-at-a-time, which metric (e.g., 1-day, 3-day, 5-day, or 7-day total rainfall) was most suitable to be included in the final nonstationary models. Preliminary models were also used to provide an early indication of which distribution parameter should vary as a function of each climate covariate. To address the issue of collinearity, covariates representing the same process (e.g., 1-day and 3-day total rainfall), which are likely correlated, were evaluated independently. Covariate suitability was determined based on nllh values between the model of interest and the stationary model. Based on these outcomes, additional models were developed by adding and combining covariates in each parameter and model performance was largely determined based on AICc scores, as most models were not nested. Quantile-Quantile (Q-Q) plots and kernel density functions of empirical vs. modelled results were also evaluated to determine the best-suited model (Slater et al., 2021). The covariates used in the final climate models indicate the dominant physical drivers of floods in each respective watershed.

Model development was carried out using R (R Core Team, 2020) and the statistical package "**extRemes**" (Gilleland & Katz, 2016). Outcomes from the full and reduced records (created by omitting four ROS events in Big Creek and a single outlier in the Deadman) were both considered during model development to (i) test for model sensitivity to floods generated by ROS events detected in Big Creek, and (ii) test for sensitivity to a single outlier in the Deadman River.

3.7. Attribution and quantification

After accounting for natural climate variability, ECA was added to the final climate model in the treatment watershed(s) to determine the effect of forest harvesting on floods. If the addition of ECA was an improvement over the final climate model, then harvesting can be deemed a driver of change to the flood distribution over the study period. Model development serves the purpose of detecting harvesting (via proxy of the ECA metric) as a potential driver of nonstationarity in the flood time series. However, the attribution of harvesting is only viable after no trends have been detected in the flood frequency distribution of the control watershed. Time is added as a covariate to the final nonstationary models to ensure that there is no remaining unexplained variability in both the control and treatment watersheds. Once this is validated, the experiment is therefore aiming at a causal inference framework. Quantiles taken from the cdf of the final nonstationary control and treatment models can then be extracted to generate a time series of exceedance probabilities, which in turn can be translated into a time series of return levels.

3.7.1. Attribution: Nonstationary return levels to validate the effect of harvesting

Return level plots, which show how the magnitude associated with a fixed return period is changing over the study period, are produced for both control and treatment watersheds. The lack of a detectible trend in the control watershed serves to elucidate any trend detected in the treatment to harvesting. In other words, if trends are detected in the return levels of the treatment watershed, but not in the control, these trends can be attributed to harvesting.

Several trend tests commonly, although often inappropriately (see Serinaldi et al., 2018), used to detect trends in observable flood records, are applied to the return level plots to confirm an increasing trend from harvesting. The Pettitt test was applied to detect any change-points in the time series, and the parametric Pearson's r, non-parametric Mann-Kendall, and Spearman's rho tests were applied to detect any monotonic trends. Helsel et al., (2020) and Villarini et al., (2009) describe the use and statistical basis of these detection tests, and Serinaldi et al., (2018) provides an in-depth discussion on the misuse of such trend tests, particularly on observed data without apriori knowledge of the underlying stochastic processes.

Applying these tests to the nonstationary return levels in this study is justified because any variability invoked by climate, which could confound results and cause unwarranted detection of nonstationarity, is accounted for by the climate covariates in the models. However, the outcomes of null hypothesis significance tests from these trend tests must still be evaluated cautiously (Serinaldi et al., 2018), given the short record length and variability within a given return period, particularly for higher return period floods. Shorter record lengths have been found to lead to a much higher occurrence of type II errors, where an upward trend exists but is not identified (e.g., Villarini et al., 2018). Furthermore, a lack of statistical significance does not necessarily warrant a lack of practical (Kirk, 1996; Serinaldi et al., 2018; Villarini et al., 2018; Yue et al., 2002) or physical (Klemeš, 1978) significance, as highlighted in sections 4 & 5 of Alila et al. (2010). Therefore, the interpretation of the outcomes of these trend tests was evaluated based on an understanding that a lack of statistical significance did not necessarily warrant a lack of practical or physical significance, provided physically plausible reasoning.

If no trends are detected in the flood frequency distribution of the control watershed but are detected in the treatment watershed, after accounting for natural climate variability and introducing ECA as a covariate into the nonstationary model, then harvesting can be attributed as a nonstationary driver of floods.

3.7.2. Quantification: Snapshot flood frequency curves at various levels of harvesting

Quantifying the effect of harvesting on floods involves modelling the distribution parameters as a function of fixed climate values representing the long-term average of each climate covariate used in the final nonstationary model while allowing the distribution parameters to change as a function of ECA. In other words, the distribution parameters are only changing as a function of the harvesting metric ECA, while the natural background signal is accounted for by the long-term average climate values (e.g., average annual peak SWE over the study period). This allows for a "snapshot in time" FFC to be generated to determine changes in magnitude and frequency invoked by changes in the mean and variability of the frequency distribution, at a specific level of harvesting. The same level of ECA can be set between the Deadman River watershed and the Joe Ross Creek sub-basin to compare forest harvesting effects in both basins, at equivalent levels of harvesting. An ECA value of 21%, representing the average ECA experienced in the Deadman River following the MPB outbreak, was arbitrarily selected to generate the snapshot FFC. Differences or similarities in the treatment effect between the Deadman River watershed and nested Joe Ross Creek sub-basin can then be related to differences in physiographies, inherently expressed by each respective FFC.

3.7.3. Uncertainty analysis

Following a similar re-sampling procedure outlined by Yu & Alila, (2019), confidence intervals for the FFCs representing undisturbed (forested) conditions were calculated via a parametric bootstrap method using the R package "**extRemes**" (Gilleland & Katz, 2016). First, a

simulated sample of floods of length n, equal to the data originally fit to the model, are randomly generated from the parent GEV distribution. Next, the sample distribution is produced by fitting the sample floods to the GEV distribution, which is used to generate the quantiles of interest. This procedure is repeated through 10,000 iterations to obtain a sample of quantiles, which can then be used to calculate confidence intervals representing the 0.05 and 0.95 quantiles of the distribution.

4. Results

4.1. Detection: Nonstationary stochastic model development to determine flood drivers using probabilistic physics

The preliminary control models for Big Creek indicated that, of the climate metrics used (e.g., 1-day, 3-day, 5-day total rainfall preceding the melt), the total 3-day rainfall and peak annual SWE provided the greatest improvement over the stationary model. Results from the likelihood ratio tests between the nonstationary and stationary models (Table 2) suggest improved model performance when the location parameter was modelled as a function of rain and/or snow, and the scale parameter modelled as a function of rain. Interestingly, time emerged as a significant covariate in the scale parameter, hinting towards the possibility of a nonstationary time series. Omitting the ROS events from the record lowered the level of significance for all preliminary models containing rainfall metrics and increased significance when the warming rate was included as a covariate (results not shown).

The final control models (CMs) were evaluated based on AICc scores and are summarized in Table 3. CM3, with the location parameter varying linearly as a function of rain (3-day rainfall) and snow (peak annual SWE), and the scale parameter varying as a function of rain, was found to be the superior model using the full record. The final model based on the reduced record had the same covariates in the location parameter; however, it performed better without the scale parameter varying as a function of rain (CM2). Models CM6-CM9 were created to assess whether any additional variability could be explained by synoptic-scale teleconnections, although they did not result in an improvement over CM2 or CM3. Finally, time was introduced as a covariate (CM10) to ensure there was no unexplained variability, which was confirmed by a likelihood ratio test between CM10 and CM1, and an increase in AICc scores for both records.

In the Deadman River watershed, preliminary treatment models suggested that peak annual SWE, total 5-day rainfall, 3-day warming rate, and daily temperature were the best metrics to be included in the final models. The treatment models in Table 2 suggest that the location parameter should primarily be modelled as a function of snow, warming rate, and/or temperature, and the scale parameter as a function of rain and/or warming rate. The synoptic-scale teleconnections also improved the variability explained by the model when the scale parameter was modelled as a function of SOI, and when both the location and scale were modelled as a function of either SOI or PDO. Time was not a significant covariate when modelled on its own; however, ECA did emerge as significant in the location parameter, albeit at the 10 % significance level.

Table 2
Preliminary models used to determine covariate suitability for the control and treatment watersheds. Model suitability is determined based on the outcomes of a likelihood-ratio test between each nonstationary model and the stationary model. Outcomes are shown for the full record lengths.

Covariate description	Model description	Control	Treatment	
		Big Creek	Deadman River	Joe Ross Creek
Stationary (no covariates)	Qp(μ, σ, ξ)			
Time (years)	Qp(μ(time), σ, ξ)	–	–	✓[c]
	Qp(μ, σ(time), ξ)	✓[b]	–	–
	Qp(μ(time), σ(time), ξ)	✓[b]	–	✓[c]
Temperature (°C) preceding the melt	Qp(μ(temp), σ, ξ)	–	✓[c]	✓[a]
	Qp(μ, σ(temp), ξ)	–	–	–
	Qp(μ(temp), σ(temp), ξ)	–	–	–
Warming rate (°C/day) preceding the melt	Qp(μ(WR), σ, ξ)	–	✓[b]	–
	Qp(μ, σ(WR), ξ)	–	✓[c]	–
	Qp(μ(WR), σ(WR), ξ)	–	✓[b]	✓[b]
Precipitation as rain (mm) preceding the melt	Qp(μ(rain), σ, ξ)	✓[a]	–	–
	Qp(μ, σ(rain), ξ)	✓[a]	✓[a]	✓[b]
	Qp(μ(rain), σ(rain), ξ)	✓[a]	✓[a]	✓[b]
Peak annual snow water equivalent (mm)	Qp(μ(snow), σ, ξ)	✓[b]	✓[a]	✓[a]
	Qp(μ, σ(snow), ξ)	–	–	✓[c]
	Qp(μ(snow), σ(snow), ξ)	✓[a]	✓[a]	✓[a]
Southern Oscillation Index	Qp(μ(SOI), σ, ξ)	–	–	–
	Qp(μ, σ(SOI), ξ)	–	✓[b]	✓[b]
	Qp(μ(SOI), σ(SOI), ξ)	–	✓[c]	✓[c]
Pacific Decadal Oscillation	Qp(μ(PDO), σ, ξ)	–	–	–
	Qp(μ, σ(PDO), ξ)	–	–	–
	Qp(μ(PDO), σ(PDO), ξ)	–	✓[b]	✓[b]
Equivalent Clearcut Area (%)	Qp(μ(ECA), σ, ξ)		✓[c]	✓[b]
	Qp(μ, σ(ECA), ξ)		–	–
	Qp(μ(ECA), σ(ECA), ξ)		–	✓[b]

- Not a significant improvement over the stationary model.
[a] Significant over the stationary model at the 99% significance level.
[b] ✓ Significant over the stationary model at the 95% significance level.
[c] Significant over the stationary model at the 90% significance level.

Table 3
Nonstationary GEV models from the final model development for the control watershed Big Creek. Reduced record (n = 36) created by omitting four large rain-on-snow events from the record. Boldfaced values indicate the model with the lowest AICc score from each record.

Model #	Model description	Full record		Reduced record	
		-Log-lik	AICc	-Log-lik	AICc
CM1	Qp(μ, σ, ξ)	173.89	354.44	141.53	289.81
CM2	Qp(μ(rain, snow), σ, ξ)	164.46[a]	340.68	133.11[a]	**278.21**
CM3	Qp(μ(rain, snow), σ(rain), ξ)	160.37[a]	**335.30**	133.10[a]	281.10
CM4	Qp(μ(rain), σ(rain, snow), ξ)	163.59[a]	341.73	136.17[b]	287.23
CM5	Qp(μ(rain, snow), σ(rain, snow), ξ)	159.31[a]	336.12	133.05[a]	284.09
CM6	Qp(μ(rain, snow, PDO), σ(rain), ξ)	160.37[a]	338.25	133.09[a]	284.18
CM7	Qp(μ(rain, snow, SOI), σ(rain), ξ)	159.90[a]	337.30	131.48[a]	280.95
CM8	Qp(μ(rain, snow), σ((rain, PDO)), ξ)	160.23[a]	337.96	133.10[a]	284.19
CM9	Qp(μ(rain, snow), σ((rain, SOI)), ξ)	160.25[a]	338.01	133.08[a]	284.15
CM10	Qp(μ(rain, snow, time), σ((rain, time)), ξ)	159.46[a]	339.56	131.74[a]	284.82

[a] Significant over the stationary model at the 99% significance level.
[b] Significant over the stationary model at the 95% significance level.

Table 4
Nonstationary GEV models from the final model development for the treatment watershed Deadman River. Reduced record (n = 39) created by omitting an anomalous high flood value. Boldface values indicate the model with the lowest AICc score from each record.

		-Log-lik	AICc	-Log-lik	AICc
Model #	Model description	Full record		Reduced record	
DM-TM1	Qp(μ, σ, ξ)	137.37	281.41	128.89	264.46
DM-TM2	Qp(μ(snow), σ(rain), ξ)	128.08[a]	267.92	120.07[a]	251.96
DM-TM3	Qp(μ(snow), σ(snow, rain), ξ)	128.07[a]	270.68	119.93[a]	254.48
DM-TM4	Qp(μ(snow, WR), σ(rain), ξ)	122.18[a]	258.90	113.87[a]	242.37
DM-TM5	Qp(μ(snow, WR, temp), σ(rain), ξ)	122.16[a]	261.83	113.87[a]	245.35
DM-TM6	Qp(μ(snow), σ(rain, WR), ξ)	128.08[a]	270.70	119.31[a]	253.24
DM-TM7	Qp(μ(snow, WR, ECA), σ(rain), ξ)	119.99[a]	**257.47**	111.72[a]	**241.05**
DM-TM8	Qp(μ(snow, WR), σ(rain, ECA), ξ)	120.47[a]	258.44	112.65[a]	242.92
DM-TM9	Qp(μ(snow, WR, ECA), σ(rain, ECA), ξ)	119.50[a]	259.64	111.63[a]	244.05
DM-TM10	Qp(μ(snow, WR, ECA, PDO), σ(rain), ξ)	119.74[a]	260.13	111.72[a]	244.24
DM-TM11	Qp(μ(snow, WR, ECA), σ(rain, PDO), ξ)	98.18[~]	217.01	81.64[~]	184.08
DM-TM12	Qp(μ(snow, WR, ECA, SOI), σ(rain), ξ)	119.74[a]	260.13	104.27[a]	229.34
DM-TM13	Qp(μ(snow, WR, ECA), σ(rain, SOI), ξ)	90.77[~]	202.19	78.99[~]	178.78
DM-TM14	Qp(μ(snow, WR, ECA, time), σ(rain, time), ξ)	118.99[a]	261.97	111.20[a]	246.61

[a] Significant over the stationary model at the 99% significance level.
[~] Indicates a lack of convergence to a non-optimum point.

Summary statistics from the likelihood ratio test between the stationary and nonstationary models and AICc scores used to develop the final nonstationary models for the Deadman River are shown in Table 4. Deadman River treatment model 2 (DM-TM2) was created based on the two dominant covariates from the preliminary analysis (Table 2), namely, with the location parameter a function of snow and the scale parameter a function of rain. Snow was added to the scale parameter although did not improve model performance (DM3-TM3). Additional models were developed incorporating warming rate and temperature as covariates (DM-TM4 to DM-TM6). However, DM-TM4 proved to be the best-suited model, with the location parameter modelled as a function of snow and warming rate, and the scale parameter a function of rain. This model is termed the "final climate model" and accounts for the natural background variability invoked by local climate factors.

Next, ECA was introduced to the final climate model (DM-TM4) to create models DM-TM7 to DM-TM9. AICc scores indicate an improvement in the variability explained by the model when the location parameter was also made a function of ECA (DM-TM7). A likelihood-ratio test between the final climate model (DM-TM4) and DM-TM7 indicates an improvement over the final climate model at the 95% significance level (p-value: 0.038). Synoptic scale teleconnections and time were then added as covariates to the final nonstationary model to ensure there was no remaining unexplained variability. Each case either resulted in a lack of convergence or an increase in AICc scores (DM-TM10 to DM-TM14). Therefore, DM-TM7 was selected as the final nonstationary model and used for the remainder of the attribution and quantification process. Using the full or reduced record did not make any difference in the final model outcomes in the Deadman River.

For Joe Ross Creek, the total 5-day rainfall, 30-day warming rate, and 3-day average temperature were determined to be the best metrics to be included in the final model development. Notable differences between the preliminary models from Joe Ross Creek and those from the Deadman River were that, for Joe Ross Creek, warming rate was only significant when modelled with both the location and scale parameter together, time became a significant covariate in the location parameter alone and in both the location and scale parameter together, and a stronger signal was detected for ECA Table 2.

The same combination of covariates used to initiate the final model development for the Deadman River was used to create the Joe Ross treatment model 2 (JR-TM2). However, the models were developed differently according to outcomes from the preliminary analysis in Table 2. The final models and associated summary statistics for Joe Ross Creek are shown in Table 5. Throughout the development of models JR-TM3 to JR-TM9, it became evident that model performance was improved when the location parameter was made a function of snow and warming rate and the scale parameter was made a function of either snow (JR-TM6) or rain (JR-TM7), but not both (JR-TM8 and JR-TM9). The final climate model was determined to be either JR-TM6 or JR-TM7, although a lack of convergence occurred when ECA was introduced to the model with the scale varying as a function of snow (JR-TM10). Interestingly, including rain in the location parameter of JR-TM11 further accounted for some unexplained variability, owing to the final nonstationary model JR-TM12. A likelihood-ratio test between JR-TM15 (the same model as JR-TM12 but without ECA) and JR-TM12 indicates that including ECA in the model is an improvement at the 95% significance level (p-value: 0.0029). Including synoptic-scale climate indices and time into the final nonstationary model did not improve

Table 5
Nonstationary GEV models used in final model development for the treatment catchment Joe Ross Creek. Boldface values indicate the model with the lowest AICc score.

Model #	Model description	-Log-lik	AICc
JR-TM1	Qp(μ, σ, ξ)	53.22	113.44
JR-TM2	Qp(μ(snow), σ(rain), ξ)	46.33[a]	105.39
JR-TM3	Qp(μ(snow), σ(snow, rain), ξ)	49.20[b]	111.12
JR-TM4	Qp(μ(snow, rain), σ(rain), ξ)	46.33[a]	108.66
JR-TM5	Qp(μ(snow, rain), σ(snow, rain), ξ)	16.43[~]	52.46
JR-TM6	Qp(μ(snow, WR), σ(snow), ξ)	42.95[a]	101.91
JR-TM7	Qp(μ(snow, WR), σ(rain), ξ)	43.26[a]	102.52
JR-TM8	Qp(μ(snow, WR), σ(WR), ξ)	19.40[~]	54.80
JR-TM9	Qp(μ(snow, WR), σ(snow, rain), ξ)	9.40[~]	38.41
JR-TM10	Qp(μ(snow, WR, ECA), σ(snow), ξ)	8.16[~]	35.92
JR-TM11	Qp(μ(snow, WR, ECA), σ(rain), ξ)	41.21[a]	102.01
JR-TM12	Qp(μ(snow, WR, rain, ECA), σ(rain), ξ)	37.97[a]	**99.53**
JR-TM13	Qp(μ(snow, WR, rain), σ(rain, ECA), ξ)	40.81[a]	105.20
JR-TM14	Qp(μ(snow, WR, rain, ECA), σ(rain, ECA), ξ)	37.79[a]	103.57
JR-TM15	Qp(μ(snow, WR, rain), σ(rain), ξ)	42.41[a]	104.42
JR-TM16	Qp(μ(snow, WR, rain, ECA, PDO), σ(rain), ξ)	37.48[a]	102.96
JR-TM17	Qp(μ(snow, WR, rain, ECA), σ(rain, PDO), ξ)	37.96[a]	103.92
JR-TM18	Qp(μ(snow, WR, rain, ECA, PDO), σ(rain, PDO), ξ)	37.45[a]	105.75
JR-TM19	Qp(μ(snow, WR, rain, ECA, SOI), σ(rain), ξ)	36.56[a]	101.12
JR-TM20	Qp(μ(snow, WR, rain, ECA), σ(rain, SOI), ξ)	37.95[a]	103.89
JR-TM21	Qp(μ(snow, WR, rain, ECA, SOI), σ(rain, SOI), ξ)	10.37[~]	53.68
JR-TM22	Qp(μ(snow, WR, rain, ECA, time), σ(rain, time), ξ)	17.21[~]	67.36

[a] Significant over the stationary model at the 99% significance level.
[b] Significant over the stationary model at the 95% significance level.
[~] Indicates a lack of convergence to a non-optimum point.

model performance, ruling out the possibility of any remaining variability in the flood distribution.

4.2. Attributing forest harvesting as a nonstationary driver of floods

Quantiles from the final nonstationary control and treatment models (CM12, DM-TM7, and JR-TM12) were extracted to produce a time series of return levels, showing how an event of a fixed frequency (e.g., the 10-year return period) is changing in magnitude over the study period. These are termed return level plots and are illustrated for the 2-, 7- and 50-year return period events in Fig. 4. A trendline can then be fit to the return level time series to determine whether there is a trend in the treatment but not in the control. The trendlines also indicate how floods of different frequencies differ in response to harvesting, by comparing the slopes of each return level trendline.

A visual inspection reveals an increasing trend in both treatment watersheds (Fig. 4b & c); however, this also appears to emerge for the 50-year return level for the control watershed Big Creek (Fig. 4a). To validate whether the apparent trend is real, a trend analysis was conducted on each of the return level time series. P-values from the trend tests are summarized in the inset table in the upper right-hand corner of each plot in Fig. 4.

Despite an apparent trend in the control watershed, the trend tests reveal no significant trend (Fig. 4a), rendering the Big Creek time series suitable as a control. Furthermore, omitting the four ROS events from the Big Creek record and re-running the analysis, caused the slope of the trendline for all return levels to flatten (Fig. 5). Comparatively, trends were detected for most return levels in the Deadman River time series, and for nearly all return levels in the Joe Ross Creek time series (Fig. 4b, c). However, the level of significance tended to decrease with increasing return period or flood magnitude. For Joe Ross Creek, trends were generally detected at higher levels of significance than in the Deadman River.

4.3. Quantifying nonstationarity invoked by harvesting

Snapshot in time FFCs are created using the final nonstationary models with their respective fixed long-term average climate covariate values while allowing the distribution parameters to vary only as a function of ECA. Only the location parameter was modelled to change with ECA since there was no improved model performance with ECA in the scale parameter. An ECA value of 21% was set for both treatment watersheds, representing the average ECA experienced in the Deadman River following the MPB outbreak. Additionally, an ECA value of zero was used to develop a curve representing the no harvest scenario.

The snapshot in time FFCs are illustrated in Fig. 6, with red arrows showing how the 7-year, 20-year, and 50-year return period events are changing in frequency from a no harvest scenario to an ECA of 21%. Changes to the mean and variability of the FFC invoked by harvesting are displayed in the upper right-hand corner of each plot. In the Deadman River, ECA levels of 21% caused the mean of the flood frequency distribution (represented in the form of an FFC), to increase relative to the no harvest scenario by 38.1%, with negligible influence on the variability (+0.3%) (Fig. 6). An increase in the mean of 38.1%, invoked by harvest levels experienced at the end of the study period, caused flood events to become 2.3 to 6.3 times more frequent, with larger increases in frequency occurring for higher magnitude flood events. A 21% ECA caused the 7-year event to become a 3-year event, the 20-year event to become a 5-year event, and the 50-year event to become an 8-year event. In Joe Ross Creek, ECA levels of 21% caused the mean to increase by 84.2%, causing the 7-year, 20-year, and 50-year flood events to increase in frequency to become less than a 2-year, 4-year, and 7-year event, respectively (Fig. 6). This translates to an increase in the frequency of the 7- and 50-year flood events by 3.9 to 7.1 times, respectively. Like the Deadman River, harvesting had a negligible effect on flood variability (+0.6%) in Joe Ross Creek.

Fig. 6 illustrates that the nested Joe Ross Creek sub-basin experienced nearly double the increase in the mean compared to the greater Deadman watershed (84.2% vs. 38.1%) with the same level of harvesting. However, with only slightly larger increases in frequency for smaller event magnitudes and nearly no difference for infrequent floods. In both treatment basins, changes in frequency increased with increasing event size. Changes in magnitude relative to the no harvest (0% ECA) scenario are expressed in Table 6 for harvest levels experienced at the end of the study period in each basin, and for an arbitrarily set ECA value of 21% (boldfaced values), to allow the comparison of harvesting effects on floods between basins.

5. Discussion

5.1. Stochastic physics reveals the effects of climatic drivers on floods

An understanding of the physical drivers of floods can be interpreted by evaluating which climatic factors emerged as dominant covariates throughout the modelling procedure. The specific parameter (e.g., location or scale) modelled as a function of each climate covariate indicates how that climatic factor is affecting floods, whereby the location and scale parameters are proxies for the mean and variability around the mean of floods, respectively.

Based on the final nonstationary model for Big Creek CM3 (Table 3), the amount of snow on the ground and rain preceding the melt emerged as the dominant flood drivers. These findings are in accordance with a linear regression-based modelling study conducted by Curry & Zwiers, (2018), who evaluated controls on floods in various catchments throughout the Fraser River Basin, BC. At Big Creek, the mean of the flood distribution was found to be related to rain and snow, and the variability a function of rain. However, after omitting the four largest floods on record (each generated by large ROS events), and re-developing the nonstationary models, rain no longer influenced flood variability (CM3). This reinforces the physical basis of the climate covariates used during the model development and suggests that during the four large ROS events, flood magnitude and particularly variability were dominantly controlled by precipitation as rain. Despite sitting at a higher elevation, the proximity of Big Creek to the coast makes it much more susceptible to ROS events compared to the treatment basins to the east. Trubilowicz & Moore (2017) found that in the coast mountains, snowmelt increased the amount of water available for runoff during large ROS events (defined as events with $>$ 40 mm of rain) by 25% on average, compared to rainfall events alone. The four largest flood events in Big Creek were associated with between 42 and 49 mm of rainfall in the three days preceding the melt and at least some rain fell within three days of the melt on 30 out of the 40 years of record. Therefore, it comes as no surprise that both the mean and variability of floods were largely influenced by rain.

In the Deadman River and Joe Ross Creek, the final nonstationary models DM-TM7 (Table 4) & JR-TM12 (Table 5) indicated that floods were dominantly controlled by the amount of snow on the ground, warming rate, and finally rain preceding the melt, consistent with the outcomes of Curry & Zwiers (2018). Unlike at Big Creek, the mean of the flood frequency distribution in the treatment basins was also influenced by increasing temperature in the days leading up to the flood event (warming rate). This difference is partially attributed to differences in slope and aspect distribution between the control and treatment basins, but more dominantly by changes in the snow-energy dynamics from the conversion of forested to unforested conditions. The emergence of warming rate in the final nonstationary treatment models further validates the physical basis of the modelling exercise. Under forested conditions, the forest canopy reduces wind which suppresses turbulent heat exchange (Harding & Pomeroy, 1996), and canopy extinction prevents shortwave radiation from reaching the below canopy snowpack (Ellis & Pomeroy, 2007; Link & Marks, 1999). The influence of canopy extinction on the snowpack is greatest on poleward-facing slopes, which

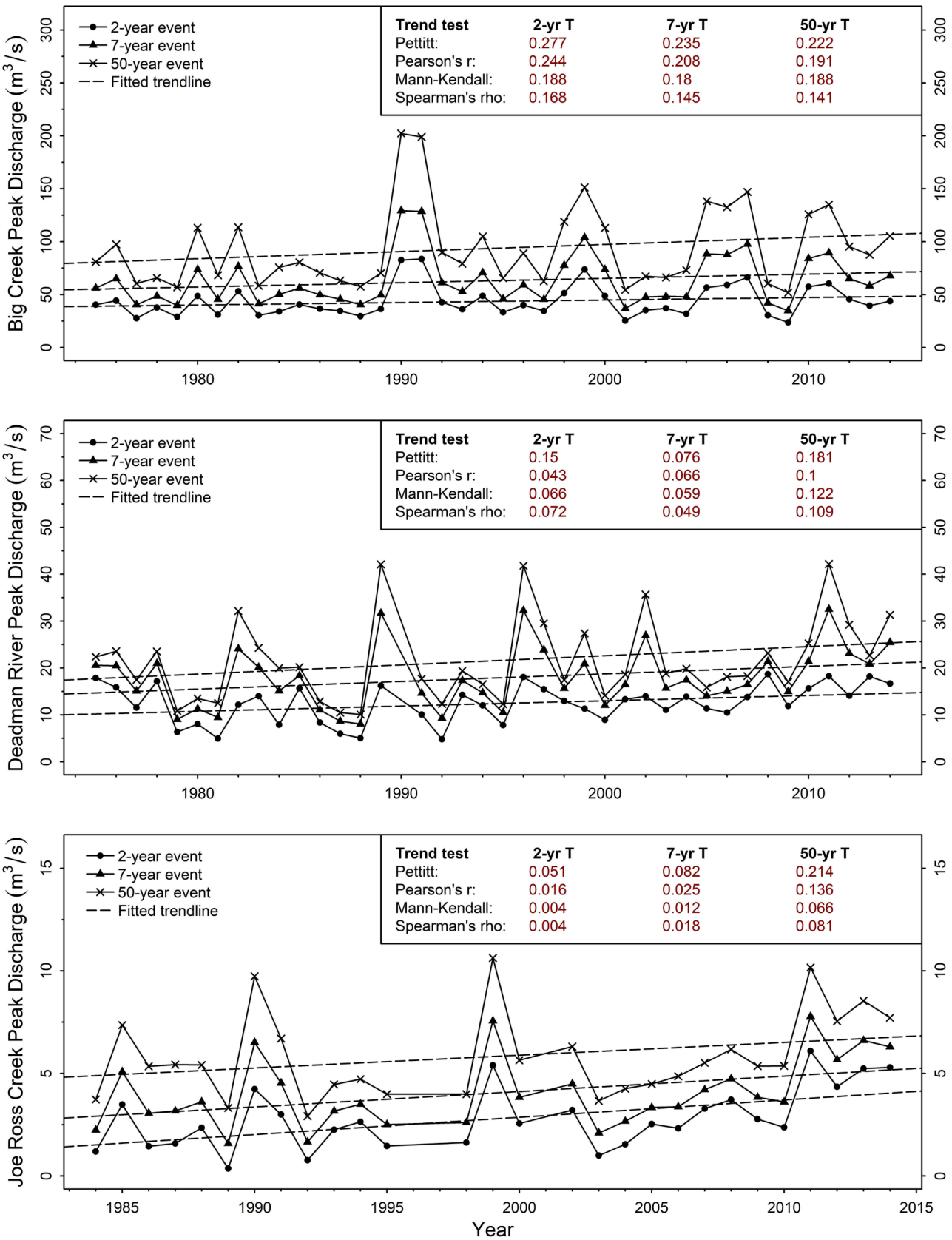

Fig. 4. Estimated 2-, 7- and 50-year return period flood magnitudes and associated trendlines over the study period, as predicted by the final nonstationary models. Numbers in red are p-values from the Pettitt change-point detection, parametric Pearson's r, and the non-parametric Mann-Kendall and Spearman's rho trend detection tests. (For interpretation of the references to color in this figure legend, the reader is referred to the web version of this article.)

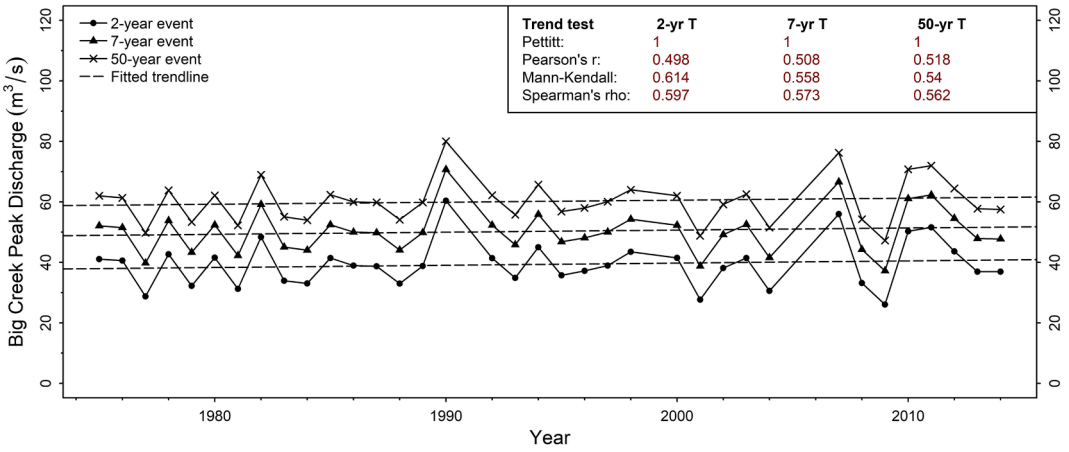

Fig. 5. Return level plot for Big Creek based on the reduced record without the four rain-on-snow events.

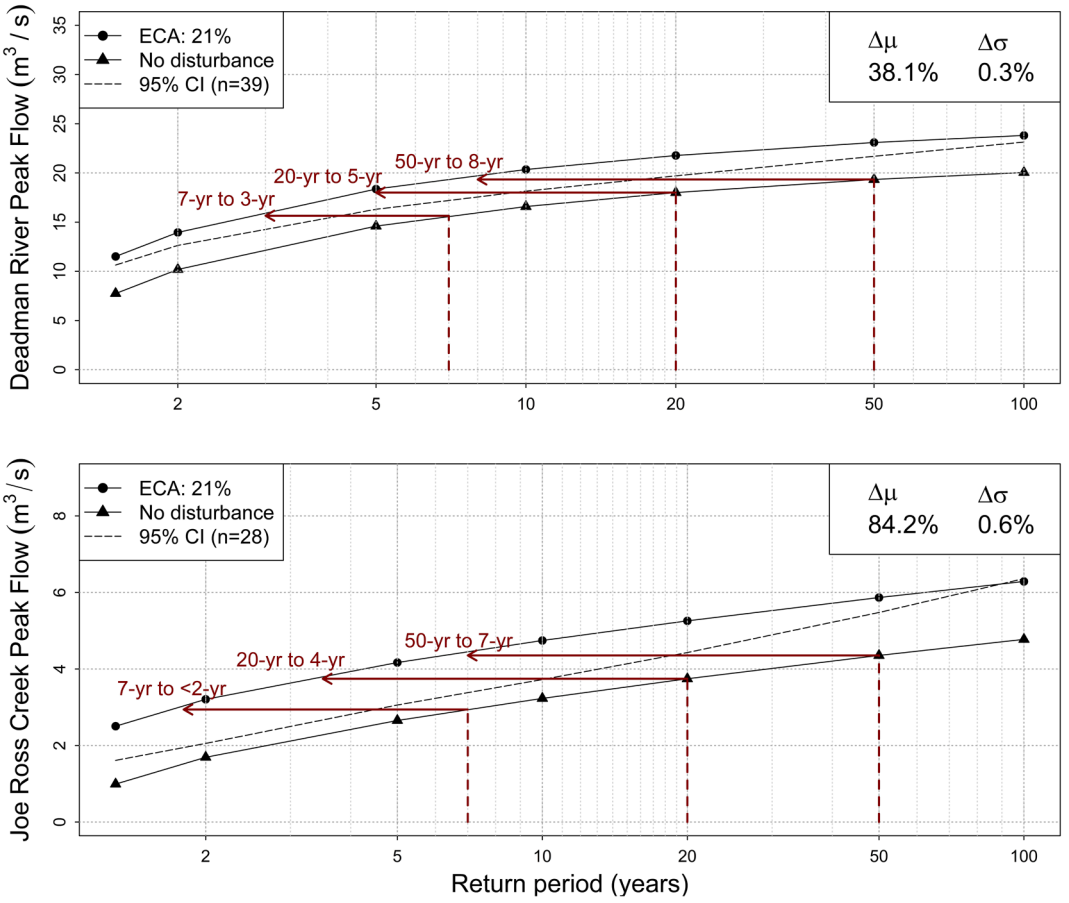

Fig. 6. Snapshot flood frequency curves from the final nonstationary models at a normalized ECA value of 21% for the Deadman River watershed (upper) and Joe Ross creek sub-basin (lower) using climate covariate values averaged over the study period. Red arrows indicate changes in frequency invoked by harvesting and the dotted black line indicates the 95% confidence interval for the no harvest FFC. Changes in the mean and variability are indicated in the upper right of each plot. (For interpretation of the references to color in this figure legend, the reader is referred to the web version of this article.)

receives greater amounts of shortwave radiation from insolation (Ellis et al., 2011). Therefore, longwave radiation emitted from vegetation to the snowpack is the dominant energy source for snowpack warming and melt under forested conditions (Black et al., 1991), particularly on north-facing aspects (Ellis et al., 2011). Big Creek has dominantly north-facing steeper slopes, whereas the treatment watersheds have either a south-dominant (Joe Ross Creek) or mixed aspect distribution (Deadman River) with subdued slopes (Fig. 2). The physiography of the treatment basins makes them much more responsive to solar radiation (Ellis et al., 2011; Jost et al., 2007; Musselman et al., 2015) and hence warming.

The conversion from forested to unforested land-cover throughout the Deadman River watershed is expected to have caused a shift from longwave to shortwave radiation-driven melt and an increase in the total net radiation reaching the snowpack (Ellis et al., 2011; Varhola et al., 2010b). Any reduction in longwave radiation with tree removal is

Table 6
Flood magnitudes at various levels of harvesting predicted by the final nonstationary models for the Deadman River (DM-TM7) and Joe Ross Creek (JR-TM12) watersheds. Percentage values in parentheses indicate the increase in flood magnitude relative to the no harvest (0% ECA) scenario. Values in boldface illustrate the changes in magnitude invoked by the same level of harvest in each treatment watershed.

Return period (years)	Deadman River flood magnitude (m^3/s)			Joe Ross Creek flood magnitude (m^3/s)		
	No harvest	**ECA 21%**	ECA 29%	No harvest	**ECA 21%**	ECA 39%
2	10.19	**13.96 (37%)**	15.45 (52%)	1.69	**3.21 (89%)**	4.47 (164%)
5	14.6	**18.36 (26%)**	19.85 (36%)	2.65	**4.17 (57%)**	5.42 (105%)
7	15.65	**19.42 (24%)**	20.91 (34%)	2.94	**4.46 (51%)**	5.72 (94%)
10	16.59	**20.35 (23%)**	21.84 (32%)	3.23	**4.75 (47%)**	6.01 (86%)
20	18.01	**21.77 (21%)**	23.26 (29%)	3.74	**5.26 (40%)**	6.52 (74%)
50	19.33	**23.10 (19%)**	24.59 (27%)	4.35	**5.87 (35%)**	7.13 (64%)
100	20.05	**23.81 (19%)**	25.30 (26%)	4.77	**6.29 (32%)**	7.54 (58%)

hypothesized to be outweighed by increases in shortwave radiation from greater insolation, resulting in earlier and more rapid melting (e.g., Zhao et al., 2021), and hence greater amounts of moisture reaching the outlet. Based on findings from a similar study by Yu & Alila (2019) in the Camp Creek watershed, roughly 200 km southeast of the Deadman River, flood variability was influenced by temperature (or warming rate) due to an acceleration of the melt with the conversion from longwave- to shortwave-dominated snowmelt following harvest. However, in the treatment watersheds of this study, warming rate was found only to be related to the location parameter in the final nonstationary models, despite early indications from the preliminary models of an influence on flood variability (Table 2). It is hypothesized that any influence of warming rate on flood variability was buffered by the melt pattern induced by the basin physiography and abundant lakes distributed throughout both treatment basins. Therefore, warming rate is expected to have only affected the mean of the flood distribution by increasing the amount of moisture reaching the outlet during flood events.

Rainfall was also found to play a role in the variability of floods at Deadman River and in both the mean and variability of floods at Joe Ross Creek. Relative to Big Creek, the quantity of rain and the number of years that experienced rainfall in the days leading up to the melt was much lower in the treatment basins. Furthermore, the 5-day rainfall, rather than the 3-day rainfall in Big Creek, was found to be the dominant rainfall metric. This suggests that rainfall dominantly acts as a snow ripening agent in the treatment basins in the week or so leading up to the peak flood date, thereby increasing the variability in runoff response in years when only significant rainfall has occurred. Flood variability by rain may not have been buffered by the lake systems due to rain falling at lower elevations below the snowline and on portions of the catchments downstream of the lakes. The influence of rain on the mean of floods in Joe Ross Creek but not in the larger Deadman River could be due to its smaller basin area. Rain events in the spring are more likely to uniformly cover the smaller Joe Ross Creek, which may otherwise be attenuated by the larger catchment area of the Deadman River (Blöschl & Sivapalan, 1997).

Interestingly, indices of PDO and ENSO did not emerge as dominant predictors of floods in either control or treatment basins, despite indications to the contrary from the preliminary models (Table 2). It is hypothesized that the signal of local climate factors on floods in the study basins is stronger than the signal from synoptic-scale teleconnections. This could be due to the correlation between the teleconnections and the local climate factors (e.g., snow, temperature, rain) driving floods in each basin (Thorne & Woo, 2011). Additionally, the 28- and 40-year flood records may have been too short to fully capture the influence of PDO, which oscillates between positive and negative phases at a frequency of 20–30 years (Mantua & Hare, 2002).

5.2. *Stochastic physics reveals the effects of forest harvesting on floods*

Much like the evaluation of climate covariates in the previous section, the influence of ECA on the flood frequency distribution can be used in conjunction with the current understanding of stand- and watershed-scale physics to infer how harvesting has affected floods in the treatment basins. In interior BC, forest harvesting generally causes an increase in snow accumulation with reduced canopy interception and an increase in snow ablation rate from increased energy input to the snowpack via solar radiation (e.g., Bewley et al., 2010; Winkler et al., 2014) and turbulent heat exchange (Boon, 2009). As mentioned previously, the removal of forest cover typically causes a shift from longwave-dominated snowmelt under forested conditions (Black et al., 1991) to shortwave-dominated melt in unforested conditions (Ellis et al., 2011; Ellis & Pomeroy, 2007). These stand-level effects translate to greater moisture availability at the catchment scale in the spring and can cause earlier melting (Winkler et al., 2015), although responses vary depending on watershed slope and aspect (Ellis et al., 2011; Jost et al., 2007).

Green & Alila (2012) proposed a conceptual model (Green & Alila, 2012; Figure 7, p.17) to illustrate how changes in the flood frequency distribution can be used to infer the influence of basin characteristics on harvesting induced changes in stand-level snow and melt processes, and how these changes are aggregated as a watershed-scale response at the outlet. They proposed that the conversion from longwave to shortwave-dominated snowmelt following harvesting caused the mean (location parameter) of the flood frequency distribution to increase. Such an increase in the mean is indicative of an increase in the amount of moisture available for runoff due to increased snow in the spring following harvest (e.g., Bewley et al., 2010; Winkler et al., 2014) and potential increases in snowmelt synchronization caused by the spatial distribution of cutblocks. Changes in the variability (scale parameter) of the distribution were interpreted as a change in the efficiency by which water is delivered to the outlet. In snow environments, Green & Alila (2012) posited that changes in the variability were caused by snowmelt synchronization or desynchronization induced by the spatial distribution of harvesting across aspect and elevation, and between snowpack in cutblocks versus neighboring forested stands. A stochastic understanding of synchronization/desynchronization processes has been applied in the rain environment outside of forest hydrology, where environmental controls such as basin geometry (e.g., Ayalew & Krajewski, 2017) and basin size (e.g., Blöschl & Sivapalan, 1997) influence runoff synchronization/desynchronization at the outlet. In snow environments, elevation and the distribution of slope and aspect, have been shown to influence the synchronization and desynchronization of runoff in both the CP- (e.g., Hendrick et al., 1971) and FP-based (e.g., Schnorbus & Alila, 2013) frameworks. When topography is subdued and aspects are unevenly distributed, snowmelt is synchronized, while a larger range in elevation and/or distribution of aspects can cause snowmelt to become desynchronized. These concepts, in concert with the current understanding of harvesting induced changes to stand-level energy dynamics, formed the basis of the conceptual model created by Green & Alila (2012; Figure 7, p.17).

Previous stationary (Green & Alila, 2012) and nonstationary (Yu & Alila, 2019) frequency-based paired-watershed studies at Camp Creek, a 37 km^2 snow-dominated headwater catchment in interior BC, found that harvesting at mid-to-high elevations, particularly on south-facing aspects, caused snowmelt generated from harvested blocks to melt earlier and synchronize with melt from forested stands at lower elevations. Another FP-based study conducted in a 470 ha catchment within the

upper Penticton Creek experimental watershed found that the spatial distribution of harvesting on the subdued topography caused an increase in snowmelt synchronization, which resulted in an increase in both the mean and variability of the peak flow frequency distribution (Schnorbus & Alila, 2013).

The final nonstationary models for the Deadman River and Joe Ross Creek indicate that ECA caused an increase in the mean but not the variability of floods (Fig. 6). Similar to Green & Alila (2012), Schnorbus & Alila (2013), and Yu & Alila (2019), an increase in the mean is expected to be dominantly caused by an increase in the amount of moisture available for runoff following harvest. It is also hypothesized that an increase in net radiation, and hence snowmelt synchronization following harvest, may also increase the mean. However, unlike in previous studies (e.g., Schnorbus & Alila, 2013), harvesting did not appear to alter flood variability. It is hypothesized that the potential for harvesting to cause an increase in variability in the Deadman River and Joe Ross Creek was limited by the basin characteristics and spatial distribution of harvesting, which inhibited any potential increase in snowmelt synchronization.

The upper plateau of the Deadman River basin (including the Joe Ross Creek sub-basin), where much of the flood generating snowpack is located, has highly subdued topography (Fig. 2b), suggesting snowmelt before harvesting likely already occurred relatively synchronously. Furthermore, harvesting in both basins was evenly spatially distributed across all aspects and elevation bands, except for the low elevations along the floodplain (Fig. 2). It is posited, based on the location of the cutblocks, that harvesting may not have further induced snowmelt synchronization, and therefore did not influence flood variability. Additionally, both basins have a high abundance of lakes and wetlands (Table 1, Fig. 2a). These lakes are widespread throughout the basin and can act to attenuate flow (Chen et al., 2021a; Luo et al., 2021), dissipating any potential harvesting-induced increases in flood variability by extending flood duration (Ravazzani et al., 2014). Flood variability at Deadman River is expected to be more greatly attenuated due to the additional presence of a series of large lake systems along the main channel downstream of Joe Ross Creek. Although much larger reservoir systems can mitigate flood response (e.g., Ayalew et al., 2013, 2015; Thomas et al., 2016; Volpi et al., 2018), the effect on flood magnitude at the outlet of the Deadman River is expected to be negligible. However, an increase in flood duration (Ravazzani et al., 2014; Volpi et al., 2018) is expected to have limited any potential increases in variability (e.g., Bradley & Potter, 1992; Fig. 5 p. 2397). Despite a lack of larger lakes along the main channel, flood variability in Joe Ross Creek is still expected to be buffered by the small lakes distributed throughout the upper reaches of the basin, although to a lesser extent than in the greater Deadman River watershed. This is evident based on the apparent influence of ECA on variability during the preliminary model development for Joe Ross Creek (Table 2). The findings in this study further support the notion proposed by Green & Alila (2012) that the effects of logging on the magnitude–frequency relation is controlled not only by the cut-rate but also the physiographic characteristics of the watershed and the spatial distribution of the cutblocks.

5.3. *Differentiating between changes in land cover and climate as drivers of nonstationarity*

Nonstationary drivers, as defined by Slater et al. (2021, p.3911), are: *"longer-term processes which may cause significant shifts in the underlying distributions of hydroclimatic extremes via climate or land cover change"*. Nonstationarity invoked by climate change typically occurs over multi-decadal to millennial timescales, whereas changes in land cover can occur over much shorter periods (Slater et al., 2021). This means that nonstationarity in the flood time series may occur from climate change, land cover change, or a combination of both over the 40-year study period. The question then becomes: once a shift in the underlying flood frequency distribution has been detected, how can that shift be attributed to a single nonstationary driver? Answering this question becomes further complicated in dynamically driven systems (Trenberth et al., 2015) where causes are *multiple and chancy* (Karhausen, 2000), and the magnitude of extreme events can be compounded; multiple drivers can work either synergistically to amplify or antagonistically to buffer the response (Aghakouchak et al., 2020; Hall & Perdigao, 2021; Slater et al., 2021). Moreover, the detection of a trend may be dependent on the period of record selected (e.g., Harrigan et al., 2018).

Any changes to the flood frequency distribution invoked by a changing climate over the study period will be expressed through the climate covariates used in the nonstationary models. The climate covariates enable the effect of harvesting on floods in the treatment watershed to be isolated, but on their own do not warrant attribution. Ruling out a changing flood frequency distribution from anything other than harvesting is fundamental in controlling the experiment and enabling any change to the distribution in the treatment watersheds to be attributed to harvesting; therein lies the role of the control watershed in this new nonstationary paired watershed study design.

Despite what appears as an increase in flood return periods in Big Creek over the study period (Fig. 4), no significant trend was detected by any of the trend tests. This apparent trend is hypothesized to be an artifact of the high variability imposed by the four ROS events during the relatively short time series. This is validated by a flattening of the slope in the return level plot after the ROS events were removed from the time series (Fig. 5). Although flood trends in the control basin may be influenced by climate over longer periods (Burn & Elnur, 2002), the outcomes from the trend detection tests suggest that the flood time series can be considered stationary over the study period after accounting for the natural background variability. With no significant trend detected in the control catchment, any significant trend detected in the treatment basins can be solely attributed to forest harvesting and ruled a nonstationary driver of change to the underlying flood frequency distribution.

The return level plots for Deadman River and Joe Ross Creek (Fig. 5) indicate that floods between the 2- and 50-year return periods are increasing in magnitude over the study period. In general, lower p-values were found for trends in Joe Ross Creek compared to those in Deadman River. P-values increased (decreased in significance) with increasing return period. As mentioned in Section 3.7.1, a lack of statistical significance does not necessarily warrant a lack of practical or physical significance, provided physically plausible reasoning. Considering the severe practical consequences, and the consistency with outcomes from stationary (Alila et al., 2009; Green & Alila, 2012; Schnorbus et al., 2010; Schnorbus & Alila, 2004, 2013) and nonstationary (Yu & Alila, 2019) frequency-based studies evaluating the effect of harvesting on floods in snow-dominated catchments of B.C., the return period trends in Joe Ross Creek and Deadman River are interpreted to be highly plausible. Physical reasoning for these harvesting-induced increases in magnitude was explained in Section 5.2.

Larger (less significant) p-values for higher return period events may have occurred for two main reasons: (i) high infrequent flood variability within the relatively short record (Fig. 4), and (ii) relatively low harvest levels throughout the first 30-years of record (Fig. 3). As such, trends in higher return period events may have been obscured by the high variability. The effect of harvesting, particularly for less frequently occurring events, may have not been fully manifested in the observed flood time series and, hence, by the stochastic models during the relatively short period of increased harvest levels following the MPB outbreak in the early 2000s. Trends in higher return period events would be expected to become more distinct if a longer record were available. Additionally, lower p-values in Joe Ross Creek are posited to be associated with the higher and more rapid increase in ECA near the end of the record, and dominantly south and southwest aspects (Fig. 3).

5.4. Quantification and comparison of the effect of forest harvesting in the Deadman River basin and Joe Ross Creek sub-basin

Despite no harvesting-induced changes in the variability of the flood frequency distribution, increases in the mean caused flood events across all return periods to increase in both magnitude and frequency (Fig. 4 & Fig. 6; Table 6). At Deadman River, average harvesting levels experienced after the MPB outbreak (21% ECA) caused the mean of the frequency distribution to increase by 38.1% from no harvest conditions. This increase caused the 7-year, 20-year, and 50-year flood events to occur at a frequency of 3-years, 5-years, and 8-years, respectively (Fig. 6). At Joe Ross Creek an ECA of 21% caused an 84.2% increase in the mean, and the 7-year, 20-year, and 50-year events changed in frequency to become < 2-year, 4-year, and 7-year flood events, respectively (Fig. 6). The greater increase in the mean at Joe Ross Creek is hypothesized to have occurred due its higher median basin elevation and hence greater basin-wide snowpack, and dominantly south-facing aspect, making it much more responsive to changes in energy following harvest. Despite over twice the increase in the mean at Joe Ross Creek, increases in frequency were generally comparable in the Deadman River. The greater sensitivity of frequency from smaller increases in the mean at Deadman River is due to the shallower sloping FFC. The concept that basins with milder-sloping, or concave down, FFCs are more sensitive to harvesting was hinted at by Berris & Harr (1987, p. 141), although was not incorporated into forest hydrology research until much more recently (e.g., Alila et al., 2009; Bewley et al., 2010; Green & Alila, 2012). Green & Alila (2012) pointed out how snow environments can generally be characterized by relatively gentle-sloping FFCs. It is this inherent nature, imposed by the probabilistic physics of the snowmelt-driven flood regime, which cause relatively minor increases in magnitude, especially in the upper tail of the distribution, to cause surprisingly large changes in frequency. Greater sensitivity in the tail of the frequency distribution is a widely recognized facet in the climatology (e.g., Swain et al., 2020) and wider hydro-climatology literature:

> *"Even modest increases in the magnitude of events in the tails of the distribution can have a very substantial impact on the expected return times of events of a given magnitude."*
>
> -(Allen & Ingram, 2002; p. 229).

This phenomenon is evident in both treatment basins (Fig. 6); however, the relatively milder sloping FFC for Deadman River makes it particularly susceptible to surprisingly large changes in frequency.

Relative changes in flood magnitude invoked by an ECA of 29% (21%) at Deadman River ranged from a 52% (37%) increase for the 2-year event to a 26% (19%) increase for the 100-year event (Table 6). At Joe Ross Creek, such relative change in flood magnitude for an ECA of 39% (21%) ranged from 164% (89%) for the 2-year event to 58% (32%) for the 100-yr event (Table 6). The fact that the relative increase in magnitude becomes smaller with increasing event size has been previously used to support the notion that the influence of forest cover decreases with increasing event size (e.g., Bathurst et al., 2011; Birkinshaw et al., 2011; Jones et al., 2000). However, these relative decreases are deceptive and irrelevant (Green & Alila, 2012) as they do not convey the true influence of harvesting on larger flood events. They were reported in this study to illustrate how an evaluation of the changes in flood magnitude in relative terms is misleading. Despite smaller relative increases in magnitude, changes in frequency increase with increasing event size (Fig. 6). Furthermore, even though the Deadman River had smaller relative increases in magnitude compared to Joe Ross Creek, the shallower slope of the FFC at Deadman River dictates that these increases have a greater effect in terms of changes in frequency. In other words, the flattening of the FFC with increasing basin size causes the flood regime of larger basins to be inherently more sensitive to forest harvesting, where even modest changes in magnitude translate to large changes in frequency. Therefore, it is the absolute changes in magnitude and corresponding changes in frequency which are of scientific, physical, and practical relevance.

The changes in frequency reported for both basins in this study are substantive, and if true, can have considerable physical and practical downstream consequences. Furthermore, there appeared to be no return period threshold beyond which forest harvesting did not affect floods, and the sensitivity to harvest increased with increasing flood event size and basin area (Fig. 6). Despite running counter to the prevalent deterministic CP-based perception of forests and floods, these findings are less surprising when evaluated as part of the wider stochastic hydrology literature. Frequency-based studies from the wider hydrology community (e.g., Brath et al., 2006; Castellarin & Pistocchi, 2012; Duncan, 1995; Hurkmans et al., 2009; Kay et al., 2006; Lavigne et al., 2004; Modrick & Georgakakos, 2015; Pall et al., 2011; Preti et al., 2011; Reynard et al., 2001; Siriwardena et al., 2006; Svoboda, 1991; Te Linde et al., 2010; Zhang et al., 2018), illustrate the sensitivity of the upper tail of the flood frequency distribution to changes in climate and/or land cover. For example, a study conducted in five small rain-dominated catchments near Nelson, New Zealand, compared measured flood frequency curves for pine and pasture land and reported a roughly 50% increase in magnitude for the 50-year return period flood event, corresponding to a ten-fold increase in frequency (Duncan, 1995; Fig. 5, p. 23). Reynard et al. (2001) investigated the implications of increasing forest cover to mitigate increased flood risk associated with climate change in two large (>9,000 km^2) watersheds in the United Kingdom. The authors reported greater proportional increases in modelled flood frequency for extreme flood events (Reynard et al., 2001, p. 357).

What may be most remarkable is that substantive changes in frequency for large events can be induced by even modest increases to the mean, which may be further amplified by increases in variability. This is an established fact among hydro-climatologists (Katz, 1993; Katz & Brown, 1992; Schaeffer et al., 2005; Wigley, 1985, 2009). To illustrate this phenomenon, outcomes from several stochastic hydrology studies are showcased in Table 7. As an example, as little as a 30% increase in the mean and a 1% increase in the variability of the frequency distribution caused the 20-year flood event to double in frequency (Green & Alila, 2012). Large flood events can be affected by changes to the mean as an increase in the mean causes the entire frequency distribution to shift upwards. This increase is not limited to smaller events and is manifested throughout the entire FFC, which can be further exacerbated by an increase in variability. Greater sensitivity in the upper tail of the FFC occurs from either a divergence (increase in the variability) or parallelism (increase in only the mean) in the frequency curves for the pre-and post-land cover or climate change scenarios. In the context of forest hydrology research, observed and simulated records in both rain and snow regimes have produced diverging or parallel running FFCs which can persist up to the 100-year event for a snow regime (Kuraś et al., 2012; Fig. 5 p.9; Schnorbus and Alila, 2004, 2013; Fig. 9, p. 10, Schnorbus & Alila, 2013; Fig. 6, p. 525), and up to the 1000-year event for a rain regime (Birkinshaw et al., 2011; Figure 8 p. 1292). Any indication of convergence has been shown to be an artifact of sample size (e.g., Alila et al., 2009; Green & Alila, 2012; Kuraś et al., 2012; Schnorbus & Alila, 2013), suggesting that the no-effect threshold may persist indefinitely. A concept that is diametrically opposite to the dominant CP-based wisdom on forests and floods.

Harvesting in the Deadman River and Joe Ross Creek basins only caused an increase in the mean with minimal influence on the variability of floods. This results in parallel-running pre-and post-harvest FFCs (Fig. 6). Although changes in frequency in this study have only been reported up to the 50-year return period flood event, considering outcomes from the studies mentioned above, it is expected that the harvesting effect on floods extends beyond the 50-year return period. Fig. 6 suggests that in both treatment basins, an ECA of 21% caused the 100-year flood event to increase in frequency by roughly ten times. Moreover, taken in the context of previous FP-based studies, the substantive changes in frequency, induced by harvesting in the Deadman River and

Table 7
Stochastic hydrology studies illustrate that only moderate changes in the mean and variability are required to induce substantive changes in frequency for large events. In cases where changes in the mean and/or variability were not explicitly reported, qualitative values were assigned (e.g., minor increase/decrease).

Author	Climate regime	Data type	Land-use change	Δ mean	Δ variability	Effect on flood frequency
Alila et al. (2009)[a]	Snow	Empirical	40% area harvested	+30%	–23%	Δ from 30 yr to 14 yr event
Birkinshaw et al. (2011)	Rain	Simulated	100% forested area harvested	< than a 2x increase	Minor increase	4x increase in 100 yr event, nearly 10x increase in 1000 yr event
Duncan (1995)	Rain	Empirical	Comparison between pasture and pine-covered catchments	3x increase	Minor increase	10x increase in 50-year event
Green & Alila (2012)	Snow	Empirical	33% to 40% area harvested in four catchments	+35%, +23%, +15%, +11%	+1%, −12%, +19%, +18%	Δ from 20 yr to 10 yr, 50 yr to 13 yr
Kuraś et al. (2012)	Snow	Simulated	50% area harvested	+9%	Minor increase	5–6.7x increase in 100 yr event
Reynard et al. (2001)	Rain	Simulated	Afforestation to mitigate climate change impacts	−10%	Minor decrease	10x decrease in 50 yr event
Schnorbus & Alila (2013)	Snow	Simulated	50% area harvested	+21%	+13%	20x increase in 100 yr event

[a] Only values for the 48-year record at Fools Creek were reported.

Joe Ross Creek basins across all return periods, are highly plausible.

The lack of converging FFCs can be explained by: (i) the inextricable relation between frequency and magnitude, where one cannot change without changing the other; (ii) the dependency of subsequent event-ranking (rank is a surrogate of frequency), where a change to a single event magnitude cannot occur without influencing the subsequently ranked events; and (iii) harvesting induced changes to stand and watershed-scale physics. As a reminder, floods are *multiple and chancy* (Karhausen, 2000, p. 59), whereby the flood frequency distribution is conditional on the probability distribution of each flood driver (e.g., snow, warming rate, rain, etc.). If harvesting causes a shift in the frequency distribution of one or more flood drivers, for example, an increase in the frequency of years with higher moisture input (increased snowpack), higher energy input (increased insolation), and a higher likelihood of snowmelt synchronization, there will be an increased likelihood that a year with even a modest snowpack coincides with that of a high warming rate. This translates to an increased likelihood for large flood events to be generated by years with a relatively shallow snowpack. This is further supported by Curry & Zwiers (2018) who found that some of the largest flood events in the Fraser River basin did not always coincide with the highest snowpack years. A similar argument was articulated by Alila & Green (2014) and Duncan (1995) for rain environments, suggesting that medium magnitude rain events falling on high AMC conditions accounted for the increase in frequency for high return period flood events. Annual maximum rainfall events do not always generate the annual maximum flood peaks (e.g., Kim et al., 2019; Preti et al., 2011). For example, Kim et al. (2019) found that a 7-year precipitation event falling on saturated soils could generate a 100-year flood, whereas a 200-year precipitation event falling on unsaturated soils may only result in a 15-year flood event.

6. Conclusion

Drawing on the emerging advances in nonstationary frequency analysis and attribution science, this study sought to further the development of a new stochastic analysis approach to detect, attribute, and quantify the effect of forest harvesting on floods in interior BC. Moreover, this study sought to further the application of stochastic physics to evaluate the environmental controls and drivers of flood response and contribute to the growing science of attribution, which has a history of being handled, even in the wider hydrology literature, "*rather sloppily*" (Merz et al., 2012, p. 1385).

Conventionally restricted to small experimental watersheds, the new role of the control watershed in nonstationary paired watershed analysis has enabled the size and proximity constraints of the control and treatment watersheds to be relaxed. This has enabled larger watersheds of more practical scales to be investigated in a controlled experimental setting for the first time in main-stream forest hydrology.

Based on the final nonstationary models, floods in the Big Creek control watershed were found to be dominantly driven by the amount of snow on the ground and rain in the days leading up to the time of the peak of the freshet hydrograph. In the Deadman River and Joe Ross Creek treatment basins, floods were driven by the amount of snow on the ground, rain, and the warming rate. The greater influence of warming rate on floods in the treatment basins is thought to be caused by the conversion from longwave-to shortwave-dominated snowmelt following harvest.

Due to the even aspect distribution, even spatial distribution of cutblocks, and abundance of lakes throughout the Deadman River watershed, forest harvesting only influenced the mean of the flood frequency distribution. This was expressed by an upward shift of the flood frequency curve thought to represent an increase in the amount of moisture available for melt caused by a deeper snowpack and an increase in the amount of energy reaching the snowpack following harvest. Harvesting is not thought to have induced snowmelt synchronization, or if it had, was buffered by the abundant lakes throughout the watershed, and therefore did not influence the variability of the flood frequency distribution.

Despite no influence on the variability, harvesting-induced changes to the mean caused substantive changes in frequency. Contrary to outcomes from conventional CP-based studies on forests and floods, the effect of forest harvesting did not appear to decrease with increasing event and basin size. An ECA of 21% caused the mean of the flood frequency distribution to increase relative to fully forested conditions by 38.1% and 84.2% at Deadman River and Joe Ross Creek, respectively. Consequently, the 7-year, 20-year, and 50-year flood events increased in frequency by approximately two, four, and six times in the Deadman River, and by four, five, and seven times in Joe Ross Creek, respectively. Additionally, a 21% ECA is expected to have caused the 100-year flood event to become approximately ten times more frequent in both basins.

Forest harvesting caused changes in frequency to be greater for larger events. Additionally, smaller increases in the mean were required to induce similar changes in frequency for the larger (Deadman River) versus the smaller (Joe Ross Creek) basin. The relatively high sensitivity to harvest is dominantly due to the shallow-sloping FFC, characteristic of snowmelt-driven flood regimes (Green & Alila, 2012), which become milder in slope as basin size increases (Beckers et al., 2002; Blöschl & Sivapalan, 1997). It is this inherent nature, imposed by the probabilistic physics of the snowmelt-driven flood regime, which causes relatively minor increases in magnitude, especially in the upper tail of the distribution, to cause surprisingly large changes in frequency, a widely recognized precept among hydro-climatologists (Allen & Ingram, 2002

and references therein). Such sensitivity is a physically and practically important facet to the forest and flood relation that can only be revealed under a stochastic framework. The findings in this study further support the notion proposed by Green & Alila (2012) that the effects of logging on the magnitude–frequency relation is controlled not only by the harvest rate but also the physiographic characteristics of the watershed and the spatial distribution of the cutblocks.

The greatest limitation to this study is the relatively short flood record. However, taken in a *meta*-analysis context with previous FP-based studies (e.g., Alila et al., 2009; Duncan, 1995; Green & Alila, 2012; Kuraś et al., 2012; Reynard et al., 2001; Schnorbus & Alila, 2013), the impact of harvesting on the most extreme floods making up the upper tail of the frequency distribution must be taken as highly plausible. Due to the esoteric nature of the statistics of extremes, only modest increases in the mean are required to induce surprisingly large changes in frequency (Katz, 1993; Katz & Brown, 1992; Wigley, 2009). Therefore, substantive changes in frequency are posited to occur even within the wide range of error associated with the model predicted changes in magnitude as a direct consequence of a relatively mild sloping and concave down flood frequency curve.

The nonstationary approach to paired watershed studies enables a more realistic evaluation of the temporal evolution of harvesting in a watershed, by accounting for staggered harvesting practices over time, and subsequent forest regeneration following harvest which is of use to forest managers for future forest development planning. Moreover, once a suitable control watershed is established, it could be used for multiple opportunistic treatment basins within the same hydroclimate regime.

Additional suggestions for future studies include: 1) increasing the sample size by developing deterministic hydrologic models to corroborate or refute the predictions of observational non-stationary frequency analyses of the effect of logging on floods (e.g., Birkinshaw et al., 2011); 2) using Monte Carlo experiments to investigate the relations between covariates and the GEV, or any other alternative distribution, parameters; 3) allowing the shape parameter to be nonstationary, particularly given that recent studies have demonstrated that forest harvesting may cause the shape parameter to change over time (e.g., McEachran et al., 2021); 4) applying this method to experimental watersheds which have previously been evaluated under the stationarity assumption; 5) evaluating additional opportunistic watersheds which have not been previously investigated in a controlled experimental setting; and 6) extending the application to evaluate other forms of natural and anthropogenic disturbances, such as wildfires, insect infestations, roads, and other silviculture practices (e.g., re/afforestation), and on other flow metrics such as low flows.

Declaration of Competing Interest

The authors declare that they have no known competing financial interests or personal relationships that could have appeared to influence the work reported in this paper.

Data availability

Data will be made available on request.

Acknowledgments

We thank four referees for their detailed and thoughtful comments on earlier drafts. Their feedback challenged us and helped bolster our understanding on the application of stochastic physics as a tool to further our understanding of forest hydrology. The authors thank Peter Marshall and Steven Weijs for their feedback provided throughout the development of the manuscript. We would also like to thank Joe Yu and Jangar Tsembel for many hours spent brainstorming ideas and their valuable thought-provoking discussion, suggestions and support throughout. The authors thank Hunter Rigatti for providing editing support in the response to reviewers. We acknowledge Water Survey of Canada, Meteorological Survey of Canada, and BC Ministry of Forests, Lands, Natural Resource Operations & Rural Development for the hydrometric, climate, and vegetation inventory data sets used in our study.

Funding

This research did not receive any specific grant from funding agencies in the public, commercial, or not-for-profit sectors.

References

Aghakouchak, A., Chiang, F., Huning, L.S., Love, C.A., Mallakpour, I., Mazdiyasni, O., Moftakhari, H., Papalexiou, S.M., Ragno, E., Sadegh, M., 2020. Climate extremes and compound hazards in a warming world. Annual Review of Earth and Planetary Sciences 48, 519–548. https://doi.org/10.1146/annurev-earth-071719-055228.

Alexander, R.B., Boyer, E.W., Smith, R.A., Schwarz, G.E., Moore, R.B., 2007. The role of headwater streams in downstream water quality. Journal of the American Water Resources Association 43 (1), 41–59. https://doi.org/10.1111/j.1752-1688.2007.00005.x.

Alfieri, L., Feyen, L., Di Baldassarre, G., 2016. Increasing flood risk under climate change: a pan-European assessment of the benefits of four adaptation strategies. Climatic Change 136 (3–4), 507–521. https://doi.org/10.1007/s10584-016-1641-1.

Alila, Y., Green, K.C., 2014a. Comment on "a paradigm shift in understanding and quantifying the effects of forest harvesting on floods in snow environments" by Kim C. Green and Younes Alila. Water Resources Research 50 (3), 2765–2768. https://doi.org/10.1002/2013WR013586.

Alila, Y., Green, K.C., 2014b. Reply to comment by Bathurst on "'A paradigm shift in understanding and quantifying the effects of forest harvesting on floods in snow environments".'. Water Resources Research 50, 2759–2764. https://doi.org/10.1029/eo066i003p00017-03.

Alila, Y., Kuraś, P.K., Schnorbus, M., Hudson, R., 2009. Forests and floods: A new paradigm sheds light on age-old controversies. Water Resources Research 45 (8), 1–24. https://doi.org/10.1029/2008WR007207.

Alila, Y., Hudson, R., Kuraś, P.K., Schnorbus, M., Rasouli, K., 2010. Reply to comment by Jack Lewis et al. on "Forests and floods: A new paradigm sheds light on age old controversies". Water Resources Research 46 (5). https://doi.org/10.1029/2009WR009028.

Allen, M.R., Ingram, W.J., 2002. Constraints on future changes in climate and the hydrologic cycle. Nature 419 (6903), 224–232.

Anderson, D.R., Burnham, K.P., 2002. Avoiding pitfalls when using information-theoretic methods. The Journal of Wildlife Management 66 (3), 912–918.

Andréassian, V., Lerat, J., Le Moine, N., Perrin, C., 2012. Neighbors: Nature's own hydrological models. Journal of Hydrology 414–415, 49–58. https://doi.org/10.1016/j.jhydrol.2011.10.007.

Ashley, S.T., Ashley, W.S., 2008. Flood fatalities in the United States. Journal of Applied Meteorology and Climatology 47 (3), 805–818. https://doi.org/10.1175/2007JAMC1611.1.

Ayalew, T.B., Krajewski, W.F., 2017. Effect of river network geometry on flood frequency: A tale of two watersheds in Iowa. Journal of Hydrologic Engineering 22 (8), 06017004. https://doi.org/10.1061/(asce)he.1943-5584.0001544.

Ayalew, T.B., Krajewski, W.F., Mantilla, R., 2013. Exploring the rffect of reservoir storage on peak discharge frequency. Journal of Hydrologic Engineering 18 (12), 1697–1708. https://doi.org/10.1061/(asce)he.1943-5584.0000721.

Ayalew, T.B., Krajewski, W.F., Mantilla, R., 2015. Insights into expected changes in regulated flood frequencies due to the spatial configuration of flood retention ponds. Journal of Hydrologic Engineering 20 (10), 04015010. https://doi.org/10.1061/(asce)he.1943-5584.0001173.

Bathurst, J.C., Birkinshaw, S.J., Cisneros, F., Fallas, J., Iroumé, A., Iturraspe, R., Novillo, M.G., Urciuolo, A., Alvarado, A., Coello, C., Huber, A., Miranda, M., Ramirez, M., Sarandón, R., 2011. Forest impact on floods due to extreme rainfall and snowmelt in four Latin American environments 2: Model analysis. Journal of Hydrology 400 (3–4), 292–304. https://doi.org/10.1016/j.jhydrol.2010.09.001.

Bathurst, J.C., Fahey, B., Iroumé, A., Jones, J., 2020. Forests and floods: Using field evidence to reconcile analysis methods. Hydrological Processes 34 (15), 3295–3310. https://doi.org/10.1002/hyp.13802.

Bathurst, J.C., 2014. Comment on "'A paradigm shift in understanding and quantifying the effects of forest harvesting on floods in snow environments"' by K. C. Green and Y. Alila. Water Resources Research 50 (3), 2756–2758. https://doi.org/10.1111/j.1752-1688.1969.tb04897.x.

Beckers, J., Alila, Y., Mtiraoui, A., 2002. On the validity of the British Columbia Forest Practices Code guidelines for stream culvert discharge design. Canadian Journal of Forest Research 32 (4), 684–692. https://doi.org/10.1139/x02-010.

Berghuijs, W.R., Aalbers, E.E., Larsen, J.R., Trancoso, R., Woods, R.A., 2017. Recent changes in extreme floods across multiple continents. Environmental Research Letters 12 (11), 114035.

Berris, S.N., Harr, R.D., 1987. Comparative snow accumulation and melt during rainfall in forested and clear-cut plots in the Western Cascades of Oregon. Water Resources Research 23 (1), 135–142. https://doi.org/10.1029/WR023i001p00135.

Bertola, M., Viglione, A., Vorogushyn, S., Lun, D., Merz, B., Blöschl, G., 2021. Do small and large floods have the same drivers of change? A regional attribution analysis in

Europe. Hydrology and Earth System Sciences 25 (3), 1347–1364. https://doi.org/10.5194/hess-25-1347-2021.
Beschta, R.L., Pyles, M.R., Skaugset, A.E., Surfleet, C.G., 2000. Peakflow responses to forest practices in the western cascades of Oregon, USA. Journal of Hydrology 233 (1–4), 102–120. https://doi.org/10.1016/S0022-1694(00)00231-6.
Bewley, D., Alila, Y., Varhola, A., 2010. Variability of snow water equivalent and snow energetics across a large catchment subject to Mountain Pine Beetle infestation and rapid salvage logging. Journal of Hydrology 388 (3–4), 464–479. https://doi.org/10.1016/j.jhydrol.2010.05.031.
Biederman, J.A., Somor, A.J., Harpold, A.A., Gutmann, E.D., Breshears, D.D., Troch, P.A., Gochis, D.J., Scott, R.L., Meddens, A.J.H., Brooks, P.D., 2015. Recent tree die-off has little effect on streamflow in contrast to expected increases from historical studies. Water Resources Research 1–15. https://doi.org/10.1002/2015WR017401. Received.
Birkinshaw, S.J., Bathurst, J.C., Iroumé, A., Palacios, H., 2011. The effect of forest cover on peak flow and sediment discharge-an integrated field and modelling study in central-southern Chile. Hydrological Processes 25 (8), 1284–1297. https://doi.org/10.1002/hyp.7900.
Birkinshaw, S.J., 2014. Comment on "'A paradigm shift in understanding and quantifying the effects of forest harvesting on floods in snow environments"' by Kim C. Green and Younes Alila. Water Resources Research 50, 2765–2768. https://doi.org/10.1111/j.1752-1688.1969.tb04897.x.
Black, T.A., Chen, J.-M., Lee, X., Sagar, R.M., 1991. Characteristics of shortwave and longwave irradiances under a Douglas-fir forest stand. Canadian Journal of Forest Research 21 (7), 1020–1028.
Blum, A.G., Ferraro, P.J., Archfield, S.A., Ryberg, K.R., 2020. Causal effect of impervious cover on annual flood magnitude for the United States. Geophysical Research Letters 47 (5). https://doi.org/10.1029/2019GL086480.
Blöschl, G., Sivapalan, M., 1995. Scale issues in hydrological modelling: A review. Hydrological Processes 9 (3–4), 251–290. https://doi.org/10.1002/hyp.3360090305.
Blöschl, G., Sivapalan, M., 1997. Process controls on regional flood frequency: Coefficientof variation and basin scale. Water Resources Research 33 (12), 2967–2980.
Boon, S., 2009. Snow ablation energy balance in a dead forest stand. Hydrological Processes 23, 2600–2610. https://doi.org/10.1002/hyp.
Bradley, A.A., Potter, K.W., 1992. Flood frequency analysis of simulated flows. Water Resources Research 28 (9), 2375–2385.
Bradshaw, C.J.A., Sodhi, N.S., Peh, K.S.H., Brook, B.W., 2007. Global evidence that deforestation amplifies flood risk and severity in the developing world. Global Change Biology 13 (11), 2379–2395. https://doi.org/10.1111/j.1365-2486.2007.01446.x.
Bradshaw, C.J.A., Brook, B.W., Peh, K.S., Sodhi, N.S., Ng, J., Chen, S., 2009. Flooding policy makers with evidence to save forests. *AMBIO: A Journal of the Human.* Environment 38 (2), 125–126.
Brath, A., Montanari, A., Moretti, G., 2006. Assessing the effect on flood frequency of land use change via hydrological simulation (with uncertainty). Journal of Hydrology 324 (1–4), 141–153. https://doi.org/10.1016/j.jhydrol.2005.10.001.
Burnham, K.P., Anderson, D.R., 2004. Multimodel inference: Understanding AIC and BIC in model selection. Sociological Methods and Research 33 (2), 261–304. https://doi.org/10.1177/0049124104268644.
Calder, I.R., 2007. Debate over flood-proofing effects of planting forests. Nature 450 (13), 945.
Cannon, A.J., 2010. A flexible nonlinear modelling framework for nonstationary generalized extreme value analysis in hydroclimatology. Hydrological Processes 24 (6), 673–685. https://doi.org/10.1002/hyp.7506.
Carrick, J., Abdul Rahim, M.S.A.B., Adjei, C., Ashraa Kalee, H.H.H., Banks, S.J., Bolam, F. C., Campos Luna, I.M., Clark, B., Cowton, J., Domingos, I.F.N., Golicha, D.D., Gupta, G., Grainger, M., Hasanaliyeva, G., Hodgson, D.J., Lopez-Capel, E., Magistrali, A.J., Merrell, I.G., Oikeh, I., Othman, M.S., Ranathunga Mudiyanselage, T.K.R., Samuel, C.W.C., Sufar, E.KH., Watson, P.A., Zakaria, N.N.A. B., Stewart, G., 2019. Is planting trees the solution to reducing flood risks? Journal of Flood Risk Management 12 (S2). https://doi.org/10.1111/jfr3.12484.
Castellarin, A., Pistocchi, A., 2012. An analysis of change in alpine annual maximum discharges: Implications for the selection of design discharges. Hydrological Processes 26 (10), 1517–1526. https://doi.org/10.1002/hyp.8249.
Chen, M., Papadikis, K., Jun, C., 2021a. An investigation on the non-stationarity of flood frequency across the UK. Journal of Hydrology 597 (126309), 1–12. https://doi.org/10.1016/j.jhydrol.2021.126309.
Cheng, L., AghaKouchak, A., Gilleland, E., Katz, R.W., 2014. Non-stationary extreme value analysis in a changing climate. Climatic Change 127 (2), 353–369. https://doi.org/10.1007/s10584-014-1254-5.
Christidis, N., McCarthy, M., Stott, P.A., 2020. The increasing likelihood of temperatures above 30 to 40 °C in the United Kingdom. Nature Communications 11 (1), 1–10. https://doi.org/10.1038/s41467-020-16834-0.
Coles, S. (2001). *An introduction to Statistical Modeling of Extreme Values*.
Cunderlik, J.M., Burn, D.H., 2002. Local and regional trends in monthly maximum flows in southern British Columbia. Canadian Water Resources Journal 27 (2), 191–212. https://doi.org/10.4296/cwrj2702191.
Cunderlik, J.M., Ouarda, T.B.M.J., 2009. Trends in the timing and magnitude of floods in Canada. Journal of Hydrology 375 (3–4), 471–480. https://doi.org/10.1016/j.jhydrol.2009.06.050.
Curry, C.L., Zwiers, F.W., 2018. Examining controls on peak annual streamflow and floods in the Fraser River Basin of British Columbia. Hydrology and Earth System Sciences 22, 2285–2309.
Dawdy, D.R., Gupta, V.K., 1997. Reply [to "Comment on 'Multiscaling and skew separation in regional floods' by David R. Dawdy and Vijay K. Gupta"]. Water Resour. Res. 33 (1), 273–275.
DeWalle, D.R., 2003. Forest hydrology revisited. Hydrological Processes 17 (6), 1255–1256. https://doi.org/10.1002/hyp.5115.
Dooge, J.C., 1986. Looking for hydrologic laws. Water Resources Research 22 (9S), 46S–58S.
Downton, M.W., Miller, J.Z.B., Pielke, R.A., 2005. Reanalysis of U.S. national weather service flood loss database. Nat. Hazards Rev. 6 (1), 13–22.
Du, T., Xiong, L., Xu, C.Y., Gippel, C.J., Guo, S., Liu, P., 2015. Return period and risk analysis of nonstationary low-flow series under climate change. Journal of Hydrology 527, 234–250. https://doi.org/10.1016/j.jhydrol.2015.04.041.
Duncan, M.J., 1995. Hydrological impacts of converting pasture and gorse to pine plantation, and forest harvesting, Nelson, New Zealand. Journal of Hydrology 34 (1), 15–41.
Dymond, S.F., Richardson, P.W., Webb, L.A., Keppeler, E.T., Arismendi, I., Bladon, K.D., Cafferata, P.H., Dahlke, H.E., Longstreth, D.L., Brand, P.K., Ode, P.R., Surfleet, C.G., Wagenbrenner, J.W., 2021. A field-fased experiment on the influence of stand density reduction on watershed processes at the Caspar Creek experimental watersheds in northern California. Frontiers in Forests and Global Change 4 (July), 1–19. https://doi.org/10.3389/ffgc.2021.691732.
Eagleson, P.S., 1972. Dynamics of flood frequency. Water Resources Research 8 (4), 878–898. https://doi.org/10.1029/WR008i004p00878.
El Adlouni, S., Ouarda, T.B.M.J., Zhang, X., Roy, R., Bobée, B., 2007. Generalized maximum likelihood estimators for the nonstationary generalized extreme value model. Water Resources Research 43 (3), 1–13. https://doi.org/10.1029/2005WR004545.
Ellis, C.R., Pomeroy, J.W., 2007. Estimating sub-canopy shortwave irradiance to melting snow on forested slopes. Hydrological Processes 21, 2581–2593. https://doi.org/10.1002/hyp.
Ellis, C.R., Pomeroy, J.W., Essery, R.L.H., Link, T.E., 2011. Effects of needleleaf forest cover on radiation and snowmelt dynamics in the Canadian Rocky Mountains. Canadian Journal of Forest Research 41 (3), 608–620. https://doi.org/10.1139/X10-227.
Fahey, B., Payne, J., 2017. The Glendhu experimental catchment study, upland east Otago, New Zealand: 34 years of hydrological observations on the afforestation of tussock grasslands. Hydrological Processes 31 (16), 2921–2934. https://doi.org/10.1002/hyp.11234.
Faulkner, D., Warren, S., Spencer, P., Sharkey, P., 2020. Can we still predict the future from the past? Implementing non-stationary flood frequency analysis in the UK. Journal of Flood Risk Management 13 (1), 1–15. https://doi.org/10.1111/jfr3.12582.
Fleming, S., Whitfield, P., 2010. Spatiotemporal mapping of ENSO and PDO surface meteorological signals in British Columbia, Yukon, and southeast Alaska. Atmosphere - Ocean 48 (2), 122–131. https://doi.org/10.3137/AO1107.2010.
François, B., Schlef, K.E., Wi, S., Brown, C.M., 2019. Design considerations for riverine floods in a changing climate – A review. Journal of Hydrology 574 (April), 557–573. https://doi.org/10.1016/j.jhydrol.2019.04.068.
Fulton, R. J., 1975. Surficial geology, Kamloops Lake, British Columbia; Geological Survey of Canada, Map 1384A. scale 1, 126,720.
Gilleland, E., Katz, R.W., 2016. extRemes 2.0: An Extreme Value Analysis Package in R. Journal of Statistical Software 72 (8). https://doi.org/10.18637/jss.v072.i08.
Green, K.C., Alila, Y., 2012. A paradigm shift in understanding and quantifying the effects of forest harvesting on floods in snow environments. Water Resources Research 48 (10), 1–21. https://doi.org/10.1029/2012WR012449.
Grubbs, F.E., 1950. Sample criteria for testing outlying observations. The Annals of Mathematical Statistics 21 (1), 27–58.
Hall, J., Perdigao, A.P., 2021. Who is stirring the waters? Emerging pathways could improve attribution of changes in river flow across the globe. Science 371 (6534), 1096–1097.
Harding, R.J., Pomeroy, J.W., 1996. The energy balance of the winter boreal landscape. Journal of Climate 9 (11), 2778–2787.
Harrigan, S., Hannaford, J., Muchan, K., Marsh, T.J., 2018. Designation and trend analysis of the updated UK Benchmark Network of river flow stations: The UKBN2 dataset. Hydrology Research 49 (2), 552–567. https://doi.org/10.2166/nh.2017.058.
Hecht, J.S., Vogel, R.M., 2020. Updating urban design floods for changes in central tendency and variability using regression. Advances in Water Resources 136 (October 2019). https://doi.org/10.1016/j.advwatres.2019.103484.
Helsel, D.R., Hirsch, R.M., Ryberg, K.R., Archfield, S.A., Gilroy, E.J., 2020. Statistical methods in water resources: U.S. Geological survey techniques and methods. In: *Hydrologic Analysis and Interpretation*, p. 458.
Hendrick, R.L., Filgate, B.D., Adams, W.M., 1971. Application of environmental analysis to watershed snowmelt. Journal of Applied Meteorology 10 (3), 418–429.
Hosking, J.R.M., Wallis, J.R., 1997. *Regional frequency analysis*, p. 240.
Howe, G., Slaymaker, H., Harding, D., 1966. Flood Hazard in Mid-Wales. Nature 212 (5062), 584–585.
Hurkmans, R.T.W.L., Terink, W., Uijlenhoet, R., Moors, E.J., Troch, P.A., Verburg, P.H., 2009. Effects of land use changes on streamflow generation in the Rhine basin. Water Resources Research 45 (6), 1–15. https://doi.org/10.1029/2008WR007574.
Jones, J.A., Swanson, F.J., Wemple, B.C., Snyder, K.U., 2000. Effects of roads on hydrology, geomorphology, and disturbance patches in stream networks. Conservation Biology 14 (1), 76–85.
Jost, G., Weiler, M., Gluns, D.R., Alila, Y., 2007. The influence of forest and topography on snow accumulation and melt at the watershed-scale. Journal of Hydrology 347 (1–2), 101–115. https://doi.org/10.1016/j.jhydrol.2007.09.006.

Karhausen, L.R., 2000. Causation : The elusive grail of epidemiology. Medicine, Health Care and Philosophy 3, 59–67.
Katz, R.W., Brown, B., 1992. Extreme events in changing climate: Variability is more important than averages. Climate Change 21, 289–302. https://doi.org/10.1007/BF00139728.
Katz, R.W., Parlange, M.B., Naveau, P., 2002. Statistics of extremes in hydrology. Advances in Water Resources 25 (8–12), 1287–1304. https://doi.org/10.1016/S0309-1708(02)00056-8.
Katz, R.W., 1993. Towards a statistical paradigm for climate change. Climate Research 2 (3), 167–175. https://doi.org/10.3354/cr002167.
Katz, R.W., 2013. Statistical methods for nonstationary extremes. Extremes in a Changing Climate 65, 15–37. https://doi.org/10.1007/978-94-007-4479-0.
Kay, A.L., Jones, R.G., Reynard, N.S., 2006. RCM rainfall for UK flood frequency estimation. II. Climate change results. Journal of Hydrology 318 (1–4), 163–172. https://doi.org/10.1016/j.jhydrol.2005.06.013.
Kim, J., Johnson, L., Cifelli, R., Thorstensen, A., Chandrasekar, V., 2019. Assessment of antecedent moisture condition on flood frequency: An experimental study in Napa River Basin, CA. *Journal of Hydrology*. Regional Studies 26 (December 2018), 100629. https://doi.org/10.1016/j.ejrh.2019.100629.
Kirk, R.E., 1996. Practical significance: a concept whose time has come. Educational and Psychological Measurement 56 (5), 746–759.
Klemeš, V., 1978. Physically based stochastic hydrologic analysis. Advances in hydroscience 11, 285–356.
Kumar, N., Poonia, V., Gupta, B.B., Goyal, M.K., 2021. A novel framework for risk assessment and resilience of critical infrastructure towards climate change. Technological Forecasting and Social Change 165 (September 2020), 120532. https://doi.org/10.1016/j.techfore.2020.120532.
Kuraś, P.K., Alila, Y., Weiler, M., 2012. Forest harvesting effects on the magnitude and frequency of peak flows can increase with return period. Water Resources Research 48 (1), 1–19. https://doi.org/10.1029/2011WR010705.
Laurance, W., 2007. Forests and floods. Nature 449 (September), 409–410. https://doi.org/10.1111/j.1365-2486.2007.01446.x.
Lavigne, M.-P., Rousseau, A.N., Turcotte, R., Laroche, A.-M., Fortin, J.-P., Villeneuve, J.-P., 2004. Validation and use of a semidistributed hydrological modeling system to predict short-term effects of clear-cutting on a watershed hydrological regime. Earth Interactions 8 (3), 1–19. https://doi.org/10.1175/1087-3562(2004)008<0001:vauoas>2.0.co;2.
Lemma, T.M., Gessesse, G.D., Kassa, A.K., Edossa, D.C., 2018. Effect of spatial scale on runoff coefficient: Evidence from the Ethiopian highlands. International Soil and Water Conservation Research 6 (4), 289–296. https://doi.org/10.1016/j.iswcr.2018.08.002.
Li, J., Tan, S., 2015. Nonstationary flood frequency analysis for annual flood peak series, adopting climate indices and check dam index as covariates. Water Resources Management 29 (15), 5533–5550. https://doi.org/10.1007/s11269-015-1133-5.
Link, T.E., Marks, D., 1999. Point simulation of seasonal snow cover dynamics beneath boreal forest canopies. Journal of Geophysical Research Atmospheres 104 (D22), 27841–27857. https://doi.org/10.1029/1998JD200121.
Luo, Y., Dong, Z., Liu, Y., Zhong, D., Jiang, F., Wang, X., 2021. Safety design for water-carrying Lake flood control based on copula function: A Case study of the Hongze Lake. China. *Journal of Hydrology* 597 (March), 126188. https://doi.org/10.1016/j.jhydrol.2021.126188.
Macdonald, L.H., Stednick, J.D., 2003. Forests and water: A state-of-the-art review for Colorado Vol. 196. https://doi.org/10.4159/harvard.9780674422148.c6.
MacDonald, L.H., 2000. Evaluating and managing cumulative effects: Process and constraints. Environmental Management 26 (3), 299–315. https://doi.org/10.1007/s002670010088.
Mantua, N., Hare, S., 2002. The Pacific decadal oscillation. Journal of Oceanography 58, 35–44.
McEachran, Z.P., Karwan, D.L., Sebestyen, S.D., Slesak, R.A., Crystal Ng, G.-H., 2021. Nonstationary flood-frequency analysis to assess effects of harvest and cover type conversion on peak flows at the Marcell Experimental Forest Minnesota USA. Journal of Hydrology 596 (126054). https://doi.org/10.1016/j.jhydrol.2021.126054.
Merz, B., Vorogushyn, S., Uhlemann, S., Delgado, J., Hundecha, Y., 2012. HESS Opinions: "More efforts and scientific rigour are needed to attribute trends in flood time series". Hydrology and Earth System Sciences 16 (5), 1379–1387. https://doi.org/10.5194/hess-16-1379-2012.
Milly, P.C.D., Wetherald, R.T., Dunne, K.A., Delworth, T.L., 2002. Increasing risk of great floods in a changing climate. Nature 415 (6871), 514–517. https://doi.org/10.1038/415514a.
Milly, P.C.D., Betancourt, J., Falkenmark, M., Hirsch, R.M., Kundzewicz, Z.W., Lettenmaier, D.P., Stouffer, R.J., 2008. Climate change: Stationarity is dead: Whither water management? Science 319 (5863), 573–574. https://doi.org/10.1126/science.1151915.
Modrick, T.M., Georgakakos, K.P., 2015. The character and causes of flash flood occurrence changes in mountainous small basins of Southern California under projected climatic change. Journal of Hydrology: Regional Studies 3, 312–336. https://doi.org/10.1016/j.ejrh.2015.02.003.
Montanari, A., Koutsoyiannis, D., 2014. Modeling and mitigating natural hazards: Stationarity is immortal! Water Resources Research 50, 9748–9756. https://doi.org/10.1002/2014WR016092.Received.
Moore, R.D., McKendry, I.G., 1996. Spring snowpack anomaly patterns and winter climatic variability, British Columbia. Canada. *Water Resources Research* 32 (3), 623–632. https://doi.org/10.1029/95WR03640.
Mote, P.W., 2003. Trends in snow water equivalent in the Pacific Northwest and their climatic causes. Geophysical Research Letters 30 (12). https://doi.org/10.1029/2003GL017258.
Musselman, K.N., Pomeroy, J.W., Link, T.E., 2015. Variability in shortwave irradiance caused by forest gaps: Measurements, modelling, and implications for snow energetics. Agricultural and Forest Meteorology 207, 69–82. https://doi.org/10.1016/j.agrformet.2015.03.014.
Najafi, M.R., Zwiers, F., Gillett, N., 2017. Attribution of the observed spring snowpack decline in British Columbia to anthropogenic climate change. Journal of Climate 30 (11), 4113–4130. https://doi.org/10.1175/JCLI-D-16-0189.1.
Otto, F.E.L., Van Oldenborgh, G.J., Eden, J., Stott, P.A., Karoly, D.J., Allen, M.R., 2016. The attribution question. *Nature*. Climate Change 6 (9), 813–816. https://doi.org/10.1038/nclimate3089.
Oudin, L., Salavati, B., Furusho-Percot, C., Ribstein, P., Saadi, M., 2018. Hydrological impacts of urbanization at the catchment scale. Journal of Hydrology 559, 774–786. https://doi.org/10.1016/j.jhydrol.2018.02.064.
Pall, P., Aina, T., Stone, D.A., Stott, P.A., Nozawa, T., Hilberts, A.G.J., Lohmann, D., Allen, M.R., 2011. Anthropogenic greenhouse gas contribution to flood risk in England and Wales in autumn 2000. Nature 470 (7334), 382–385. https://doi.org/10.1038/nature09762.
Philip, S., Kew, S., van Oldenborgh, G.J., Otto, F., Vautard, R., van der Wiel, K., King, A., Lott, F., Arrighi, J., Singh, R., van Aalst, M., 2020. A protocol for probabilistic extreme event attribution analyses. Advances in Statistical Climatology, Meteorology and Oceanography 6 (2), 177–203. https://doi.org/10.5194/ascmo-6-177-2020.
Picchio, R., Jourgholami, M., Zenner, E.K., 2021. Effects of forest harvesting on water and sediment yields: A review toward better mitigation and rehabilitation strategies. Current Forestry Reports 7 (4), 214–229.
Preti, F., Forzieri, G., Chirico, G.B., 2011. Forest cover influence on regional flood frequency assessment in mediterranean catchments. Hydrology and Earth System Sciences 15 (10), 3077–3090. https://doi.org/10.5194/hess-15-3077-2011.
Price, K., Roburn, A., MacKinnon, A., 2009. Ecosystem-based management in the Great Bear Rainforest. Forest Ecology and Management 258 (4), 495–503. https://doi.org/10.1016/j.foreco.2008.10.010.
Prosdocimi, I., Kjeldsen, T.R., Miller, J.D., 2015. Detection and attribution of urbanization effect on flood extremes using nonstationary flood-frequency models. Water Resources Research 51 (3), 4244–4262. https://doi.org/10.1111/j.1752-1688.1969.tb04897.x.
Province of British Columbia. 2015. Physiographic areas. [geospatial resource: vector]. Data BC Catalogue, Victoria, BC. Retrieved from DataBC Catalogue at https://catalogue.data.gov.bc.ca/dataset/physiographic-areas.
R Core Team. 2020. R: A language and environment for statistical computing. R Foundation for Statistical Computing, Vienna, Austria. URL https://www.R-project.org/.
Ravazzani, G., Gianoli, P., Meucci, S., Mancini, M., 2014. Assessing downstream impacts of detention basins in urbanized river basins using a distributed hydrological model. Water Resources Management 28 (4), 1033–1044. https://doi.org/10.1007/s11269-014-0532-3.
Restrepo, P.J., Bras, R.L., 1985. A view of maximum-likelihood Estimation with large conceptual hydrologic models. Applied Mathematics and Computation. 17 (4), 375–403.
Reynard, N.S., Prudhomme, C., Crooks, S.M., 2001. Potential effects of changing climate and land use. Climatic Change 48, 343–359.
Salas, J.D., Rajagopalan, B., Saito, L., Brown, C., 2012. Special section on climate change and water resources: Climate nonstationarity and water resources management. Journal of Water Resources Planning and Management 138 (5), 385–388. https://doi.org/10.1061/(asce)wr.1943-5452.0000279.
Salas, J.D., Obeysekera, J., Vogel, R.M., 2018. Techniques for assessing water infrastructure for nonstationary extreme events: a review. Hydrological Sciences Journal 63 (3), 325–352. https://doi.org/10.1080/02626667.2018.1426858.
Schaeffer, M., Selten, F.M., Opsteegh, J.D., 2005. Shifts of means are not a proxy for changes in extreme winter temperatures in climate projections. Climate Dynamics 25 (1), 51–63. https://doi.org/10.1007/s00382-004-0495-9.
Schnorbus, M., Alila, Y., 2004. Forest harvesting impacts on the peak flow regime in the Columbia Mountains of southeastern British Columbia: An investigation using long-term numerical modeling. Water Resources Research 40 (5), 1–16. https://doi.org/10.1029/2003WR002918.
Schnorbus, M., Alila, Y., 2013. Peak flow regime changes following forest harvesting in a snow-dominated basin : Effects of harvest area, elevation, and channel connectivity. Water Resources Research 49 (1), 517–535. https://doi.org/10.1029/2012WR011901.
Schnorbus, M., Bennett, K., Werner, A., 2010. Quantifying the water resource impacts of mountain pine beetle and associated salvage harvest operations across a range of watershed scales: Hydrologic modelling of the Fraser River Basin. Canadian Forest Service. Information Report BC-X-423, Pacific Forestry Centre.
Schnorbus, M. (2011). A synthesis of the hydrological consequences of large-scale mountain pine beetle disturbance. In *Mountain Pine Beetle Working Paper - Pacific Forestry Centre, Canadian Forest Service* (Issues 2010–01).
Serinaldi, F., Kilsby, C.G., 2015. Stationarity is undead: Uncertainty dominates the distribution of extremes. Advances in Water Resources 77, 17–36. https://doi.org/10.1016/j.advwatres.2014.12.013.
Serinaldi, F., Kilsby, C.G., Lombardo, F., 2018. Untenable nonstationarity: An assessment of the fitness for purpose of trend tests in hydrology. Advances in Water Resources 111, 132–155.

Shepherd, T.G., 2016. A common framework for approaches to extreme event attribution. Current Climate Change Reports 2 (1), 28–38. https://doi.org/10.1007/s40641-016-0033-y.
Shrestha, R.R., Cannon, A.J., Schnorbus, M.A., Zwiers, F.W., 2017. Projecting future nonstationary extreme streamflow for the Fraser River. Canada. *Climatic Change* 145 (3–4), 289–303. https://doi.org/10.1007/s10584-017-2098-6.
Singh, N.K., Basu, N.B., 2022. The human factor in seasonal streamflows across natural and managed watersheds of North America. Nature Sustainability 5 (5), 397–405.
Singh, N., Chinnasamy, P., 2021. Non-stationary flood frequency analysis and attribution of streamflow series: a case study of Periyar River. India. *Hydrological Sciences Journal* 66 (13), 1866–1881. https://doi.org/10.1080/02626667.2021.1968406.
Siriwardena, L., Finlayson, B.L., McMahon, T.A., 2006. The impact of land use change on catchment hydrology in large catchments: The Comet River, Central Queensland. Australia. *Journal of Hydrology* 326 (1–4), 199–214. https://doi.org/10.1016/j.jhydrol.2005.10.030.
Slater, L.J., Villarini, G., 2017. Evaluating the drivers of seasonal streamflow in the U.S. Midwest. *Water (Switzerland)* 9 (695), 1–22. https://doi.org/10.3390/w9090695.
Slater, L.J., Villarini, G., 2018. Enhancing the predictability of seasonal streamflow with a statistical-dynamical Approach. Geophysical Research Letters 45 (13), 6504–6513. https://doi.org/10.1029/2018GL077945.
Slater, L.J., Anderson, B., Buechel, M., Dadson, S., Han, S., Harrigan, S., Kelder, T., Kowal, K., Lees, T., Matthews, T., Murphy, C., Wilby, R., 2021. Nonstationary weather and water extremes: a review of methods for their detection, attribution, and management. Hydrology and Earth System Sciences Discussions 25 (7), 1–54. https://doi.org/10.5194/hess-2020-576.
Stott, P.A., Stone, D.A., Allen, M.R., 2004. Human contribution to the European heatwave of 2003. Nature 432 (December), 610–613. https://doi.org/10.1029/2001jb001029.
Stott, P.A., Christidis, N., Otto, F.E.L., Sun, Y., Vanderlinden, J.P., van Oldenborgh, G.J., Vautard, R., von Storch, H., Walton, P., Yiou, P., Zwiers, F.W., 2016. Attribution of extreme weather and climate-related events. Wiley Interdisciplinary Reviews: Climate Change 7 (1), 23–41. https://doi.org/10.1002/wcc.380.
Strupczewski, W.G., Singh, V.P., Feluch, W., 2001. Non-stationary approach to at-site flood frequency modelling I. Maximum likelihood estimation. Journal of Hydrology 248 (1–4), 123–142. https://doi.org/10.1016/S0022-1694(01)00397-3.
Su, C., Chen, X., 2019. Covariates for nonstationary modeling of extreme precipitation in the Pearl River Basin, China. Atmospheric Research 229, 224–239.
Svoboda, A., 1991. Changes in flood regime by use of the modified curve number method. Hydrological Sciences Journal 36 (5), 461–470. https://doi.org/10.1080/02626669109492531.
Swain, D.L., Singh, D., Touma, D., Diffenbaugh, N.S., 2020. Attributing extreme events to climate change: A new frontier in a warming world. One Earth 2 (6), 522–527. https://doi.org/10.1016/j.oneear.2020.05.011.
Talbot, C.J., Bennett, E.M., Cassell, K., Hanes, D.M., Minor, E.C., Paerl, H., Raymond, P. A., Vargas, R., Vidon, P.G., Wollheim, W., Xenopoulos, M.A., 2018. The impact of flooding on aquatic ecosystem services. Biogeochemistry 141 (3), 439–461. https://doi.org/10.1007/s10533-018-0449-7.
Tan-Soo, J.S., Adnan, N., Ahmad, I., Pattanayak, S.K., Vincent, J.R., 2016. Econometric evidence on forest ecosystem services: Deforestation and flooding in Malaysia. Environmental and Resource Economics 63 (1), 25–44. https://doi.org/10.1007/s10640-014-9834-4.
Te Linde, A.H., Aerts, J.C.J.H., Kwadijk, J.C.J., 2010. Effectiveness of flood management measures on peak discharges in the Rhine basin under climate change. Journal of Flood Risk Management 3 (4), 248–269. https://doi.org/10.1111/j.1753-318X.2010.01076.x.
Thomas, R.B., Megahan, W.F., 1998. Peak flow responses to clear-cutting and roads in small and large basins, western Cascades, Oregon: A second opinion. Water Resources Research 34 (12), 3393–3403. https://doi.org/10.1029/98WR02500.
Thomas, N.W., Arenas Amado, A., Schilling, K.E., Weber, L.J., 2016. Evaluating the efficacy of distributed detention structures to reduce downstream flooding under variable rainfall, antecedent soil, and structural storage conditions. Advances in Water Resources 96, 74–87. https://doi.org/10.1016/j.advwatres.2016.07.002.
Thorne, R., Woo, M.K., 2011. Streamflow response to climatic variability in a complex mountainous environment: Fraser River Basin, British Columbia. Canada. *Hydrological Processes* 25 (19), 3076–3085. https://doi.org/10.1002/hyp.8225.
Trenberth, K.E., Fasullo, J.T., Shepherd, T.G., 2015. Attribution of climate extreme events. Nature Climate Change 5 (8), 725–730. https://doi.org/10.1038/nclimate2657.
Trubilowicz, J.W., Moore, R.D., 2017. Quantifying the role of the snowpack in generating water available for run-off during rain-on-snow events from snow pillow records. Hydrological Processes 31 (23), 4136–4150. https://doi.org/10.1002/hyp.11310.
Valdal, E.J., Quinn, M.S., 2011. Spatial analysis of forestry related disturbance on westslope cutthroat trout (Oncorhynchus clarkii lewisi): Implications for policy and management. Applied Spatial Analysis and Policy 4 (2), 95–111. https://doi.org/10.1007/s12061-009-9045-5.
Valentine, K.W.G., Sprout, P.N., Baker, T.E., Lavkulich, L.M., 1978. The soil landscapes of British Columbia. BC Ministry of Environment, Resource Analysis Branch, Victoria, BC.
van Dijk, van Noordwijk, M., Calder, I.R., Bruijnzeel, S.L.A., Schellekens, J.A.A.P., Chappell, N.A., 2009. Forest-flood relation still tenuous - Comment on 'Global evidence that deforestation amplifies flood risk and severity in the developing world by. Global Change Biology 15 (1), 110–115. https://doi.org/10.1111/j.1365-2486.2008.01708.x.
van Oldenborgh, G.J., van der Wiel, K., Kew, S., Philip, S., Otto, F., Vautard, R., King, A., Lott, F., Arrighi, J., Singh, R., van Aalst, M., 2021. Pathways and pitfalls in extreme event attribution. Climatic Change 166 (1–2), 1–27. https://doi.org/10.1007/s10584-021-03071-7.
Varhola, A., Coops, N.C., Bater, C.W., Teti, P., Boon, S., Weiler, M., 2010a. The influence of ground- and lidar-derived forest structure metrics on snow accumulation and ablation in disturbed forests. Canadian Journal of Forest Research 40 (4), 812–821. https://doi.org/10.1139/X10-008.
Varhola, A., Coops, N.C., Weiler, M., Moore, R.D., 2010b. Forest canopy effects on snow accumulation and ablation: An integrative review of empirical results. Journal of Hydrology 392 (3–4), 219–233. https://doi.org/10.1016/j.jhydrol.2010.08.009.
Villarini, G., Serinaldi, F., 2012. Development of statistical models for at-site probabilistic seasonal rainfall forecast. International Journal of Climatology 32 (14), 2197–2212. https://doi.org/10.1002/joc.3393.
Villarini, G., Strong, A., 2014. Roles of climate and agricultural practices in discharge changes in an agricultural watershed in Iowa. Agriculture, Ecosystems and Environment 188, 204–211. https://doi.org/10.1016/j.agee.2014.02.036.
Villarini, G., Serinaldi, F., Smith, J.A., Krajewski, W.F., 2009. On the stationarity of annual flood peaks in the continental United States during the 20th century. Water Resources Research 45 (8), 1–17. https://doi.org/10.1029/2008WR007645.
Villarini, G., Taylor, S., Wobus, C., Vogel, R. M., Hecht, J., & White, K. (2018). Floods and Nonstationarity: A review. US Army Corps of Engineers, Washington, DC. *US Army Corps of Engineers, Washington, DC*.
Volpi, E., Di Lazzaro, M., Bertola, M., Viglione, A., Fiori, A., 2018. Reservoir Effects on Flood Peak Discharge at the Catchment Scale. Water Resources Research 54 (11), 9623–9636. https://doi.org/10.1029/2018WR023866.
Vore, M.E., Déry, S.J., Hou, Y., Wei, X., 2020. Climatic influences on forest fire and mountain pine beetle outbreaks and resulting runoff effects in large watersheds in British Columbia. Canada. *Hydrological Processes* 34 (24), 4560–4575. https://doi.org/10.1002/hyp.13908.
Wang, T., Hamann, A., Spittlehouse, D., Carroll, C., 2016. Locally downscaled and spatially customizable climate data for historical and future periods for North America. PLoS ONE 11 (6), 1–17. https://doi.org/10.1371/journal.pone.0156720.
Whitaker, A., Alila, Y., Beckers, J., Toews, D., 2002. Evaluating peak flow sensitivity to clear-cutting in different elevation bands of a snowmelt-dominated mountainous catchment. Water Resources Research 38 (9), 1–17. https://doi.org/10.1029/2001wr000514.
Whitfield, P.H., Moore, R.D., Fleming, S.W., Zawadzki, A., 2010. Pacific decadal oscillation and the hydroclimatology of western canada-review and prospects. Canadian Water Resources Journal 35 (1), 1–28. https://doi.org/10.4296/cwrj3501001.
Wigley, T.M.L., 1985. Impact of extreme events. Nature 316, 106–107. https://doi.org/10.35540/903258-451.2021.8.33.
Wigley, T.M.L., 2009. The effect of changing climate on the frequency of absolute extreme events. Climatic Change 97 (1), 67–76. https://doi.org/10.1007/s10584-009-9654-7.
Winkler, R., Boon, S., 2017. Equivalent clearcut area as an indicator of hydrologic change in snow-dominated watersheds of outhern British Columbia. Government of British Columbia - Extension Note 118, 1–10.
Winkler, R., Boon, S., Zimonick, B., Spittlehouse, D., 2014. Snow accumulation and ablation response to changes in forest structure and snow surface albedo after attack by mountain pine beetle. Hydrological Processes 28 (2), 197–209. https://doi.org/10.1002/hyp.9574.
Winkler, R., Spittlehouse, D., Boon, S., Zimonick, B., 2015. Forest disturbance effects on snow and water yield in interior British Columbia. Hydrology Research 46 (4), 521–532. https://doi.org/10.2166/nh.2014.016.
Winkler, R., Spittlehouse, D., Boon, S., 2017. Streamflow response to clear - cut logging on British Columbia ' s Okanagan Plateau. Ecohydrology 10 (2), 1–15. https://doi.org/10.1002/eco.1836.
Yan, L., Li, L., Yan, P., He, H., Li, J., Lu, D., 2019. Nonstationary flood hazard analysis in response to climate change and population growth. Water (Switzerland) 11 (9), 1–20. https://doi.org/10.3390/w11091811.
Yevjevich, V., 1974. Determinisn and stochasticity in hydrology. Journal of Hydrology 22, 225–238.
Yu, X., Alila, Y., 2019. Nonstationary frequency pairing reveals a highly sensitive peak flow regime to harvesting across a wide range of return periods. Forest Ecology and Management 444 (February), 187–206. https://doi.org/10.1016/j.foreco.2019.04.008.
Yue, S., Pilon, P., Cavadias, G., 2002. Power of the Mann-Kendall and Spearman's rho tests for detecting monotonic trends in hydrological series. Journal of Hydrology 259 (1–4), 254–271. https://doi.org/10.1016/S0022-1694(01)00594-7.
Zhai, P., Zhou, B., Chen, Y., 2018. A review of climate change attribution studies. Journal of Meteorological Research 32 (5), 671–692. https://doi.org/10.1007/s13351-018-8041-6.
Zhang, X., Harvey, K.D., Hogg, W.D., Yuzyk, T.R., 2001. Trends in Canadian streamflow. Water Resources Management 37 (4), 987–998.
Zhang, W., Villarini, G., Vecchi, G.A., Smith, J.A., 2018. Urbanization exacerbated the rainfall and flooding caused by hurricane Harvey in Houston. Nature 563 (7731), 384–388. https://doi.org/10.1038/s41586-018-0676-z.
Zhang, Z., Stadnyk, T.A., Burn, D.H., 2020. Identification of a preferred statistical distribution for at-site flood frequency analysis in Canada. Canadian Water Resources Journal 45 (1), 43–58. https://doi.org/10.1080/07011784.2019.1691942.
Zhao, M., Boll, J., Brooks, E.S., 2021. Evaluating the effects of timber harvest on hydrologically sensitive areas and hydrologic response. Journal of Hydrology 593, 125805. https://doi.org/10.1016/j.jhydrol.2020.125805.